# Adaptive signal processing techniques to detect time-varying late potentials

## on a beat-to-beat basis

by

Subbaraman Narayan

A Thesis Submitted to the

Graduate Faculty in Partial Fulfillment of the

Requirements for the Degree of

MASTER OF SCIENCE

Departments: Biomedical Engineering
Electrical and Computer Engineering
Co-Majors: Biomedical Engineering
Electrical Engineering

Iowa State University
Ames, Iowa

1995

# TABLE OF CONTENTS

# LIST OF FIGURES

# ACKNOWLEDGMENTS

# CHAPTER 1.  INTRODUCTION

## 1.1  Overview

Ventricular late potentials are low amplitude, high frequency signals present in the terminal portion of the QRS of an ECG signal. These fragmented potentials are caused by the abrupt termination of the activation waveform in the electrically silent infarcted region. The non-invasive detection of these microvolt signals was first reported in 1973 [1] by using high gain amplification and ensemble signal averaging. Recent studies show that the presence of ventricular tachycardia (VT) can be quantified using late potentials [2]. It is an accepted indicator for identifying patients at risk for life threatening arrhythmias. A system which monitors these signals has a potential application in screening patients who are susceptible to various kinds of arrhythmias. Berbari was the first to demonstrate the feasibility of recording VLP's from the body surface signals [3]. He also showed a correspondence between the surface recorded signal and those signals recorded directly from the epicardial surface. As late potentials are small in comparison with the amplitude of the QRS complex, the conventional ECG is unable to detect these signals. The signal averaged electrocardiogram (SAECG) has become a widely accepted technique for risk stratification of patients. The SAECG primarily uses two signal processing techniques to process the cardiac signal for late potential analysis: time ensemble averaging; and filtering.

However there are several potential disadvantages of signal averaging. This technique cannot detect any beat-to-beat variations. This thesis presents a real time system to detect the late potentials on a beat-to-beat basis allowing assessment of dynamic changes in these signals that occur after drug therapy. The Leaky LMS algorithm is used for the enhancement of late potentials. The system is realized using a Motorola 56001 (DSP Processor). Approximately 13,000 instructions can be performed at a rate of 1 sample per millisecond. The commercially available SAECG devices average anywhere between 250-300 cycles to reduce the noise to approximately 1 microvolt. Thus at a sampling rate of 1000Hz and each QRS beat almost a second this corresponds to 4-5 minutes before the RMS values can be determined. The DSP based SAECG algorithm can be used to generate RMS values in seconds and is easily incorporated to a stand alone system. Dynamic time warping is investigated for coherent averaging. The time varying filter is also discussed as an alterative to the SAECG system.

## 1.2 Clinical Significance of Late Potentials

Several studies have evaluated the accuracy of a signal averaged ECG (SAECG) in detecting late potential's in patients with VT. It has been proved to be a non invasive technique for determination of the presence of ventricular tachycardia. The presence of late potentials has been demonstrated to be an independent risk factor for malignant ventricular arrhythmias. Surgical results can also be used to support the hypothesis that late potentials are related to damaged myocardium and ventricular tachycardia. The absence of late potentials indicates a good heart surgery. It increases the predictive accuracy for identifying survivors of acute myocardial infarc-

tion who may be at risk of sudden death. Studies by Dennis, et.al., showed that 90% of the patients (survivors of acute myocardial infarction) who subsequently developed VT had persistence of late potentials [2]. Late potentials are the signals produced during the polarization of damaged ventricular tissue. Studies have shown a correlation between late potentials and fibrillation which have made this a marker for identifying patients with life threatening arrhythmias [2].

## 1.3    Need for the Study

The SAECG has become a widely accepted technique for risk stratification of patients with potential reentrant arrhythmias. Presently six devices are commercially available in the United States for identification of late potentials. All these devices analyze the ECG by Simson's method [4]. They all employ a signal averaging algorithm. Although these devices employ a generally similar approach, totally standardized methods and criteria for the detection of late potentials have not yet been developed [2]. The results obtained from signal averaging depend on the alignment of the signals to be averaged. The average predictive accuracy is about 64% [5]. This technique does not allow the detection of dynamic changes in ventricular late potentials which may occur either spontaneously or during various diagnostic and therapeutic interventions. The clinical advantage of detecting late potentials on a beat-to-beat basis is that it facilitates the study of the relationship between late potentials and the occurrence of spontaneous or reentrant tachycardia. This thesis will focus on methods to detect late potentials on a beat-to-beat basis using adaptive filtering techniques. The following sections discuss the origin of late potentials and its clinical significance.

## 1.4  Origin of Late Potentials

Late potentials are usually found in the border zones surrounding the scar of a previous myocardial infarction [6]. The border zone that exists between scar tissue and normal tissue is composed of conducting and non-conducting tissue. Interstitial fibrosis forms in the insulating boundaries and this results in slowing and fragmentation of the wave of electrical depolarization. Therefore the border zone is both the source of late potentials and the substrate for re-entrant ventricular tachycardia.

## 1.5  Mechanism of Late Potentials

The delayed conduction that manifests itself as a 'late potential' can be caused primarily by one of two factors: slow conduction velocity or a long path length of conduction. Slow conduction velocity can be due to depressed membrane characteristics, or changes in anisotropic conduction properties caused by increased cell coupling resistances, or both. Conversely, the long path length of conduction is prolonged by tortuous conduction around regions of anatomical or functional conduction blockage. Infrequently, there is yet a third factor that can cause late potentials. Although most late potentials have been associated with depolarization of cardiac tissue, repolarization abnormalities and triggered activity can also give rise to signals that have the morphologic characteristics of late potentials. The model for reentrant excitation was proposed by Schmitt and Erlanger [7]. This model, which is based on the anatomy of a point of intersection of a Purkinje fiber and the ventricular myocardium, is equally applicable to the situation in a bundle of conducting myocardial fibers. Two properties are observed in an area of decremental conduction: Unidirectional block

and Slow conduction. In Figure 1.1 we observe that when an impulse traversing the tissue encounters the proximal end (A, Figure 1.1) of the area of decremental conduction, where antegrade conduction is blocked, the normal propagation of the impulse through the myocardium continues and the impulse is eventually conducted to a point beyond the area of decremental conduction. At this point the impulse enters the depressed area from its distal end (B), and because the block is only in the antegrade direction the impulse is able to pass through the area of decremental conduction in a retrograde direction, emerging after a delay at the proximal end (A). If the impulse has been sufficiently delayed in its passage through the area of decremental conduction, it arrives(re-enters) (A) after the normal tissue proximal to the depressed area has been recovered. In this way the second impulse is initiated in the proximal region of the myocardium that is propagated as a premature excitation. This excitation may in turn cause another excitation and through repetition of this mechanism, a run of premature excitations causes tachycardia.

## 1.6   Signal Characteristics

Late potentials are identified as low amplitude, high frequency signals which are continuous with the QRS complex and extend to the ST segment. The signal is typically characterized as being between $1 - 40\mu volts$ and comprised of frequencies in the range of 40 to 250 Hz. These micropotentials extend the duration of the QRS complex as seen in Figure 1.2 up to $120msec$ [8].
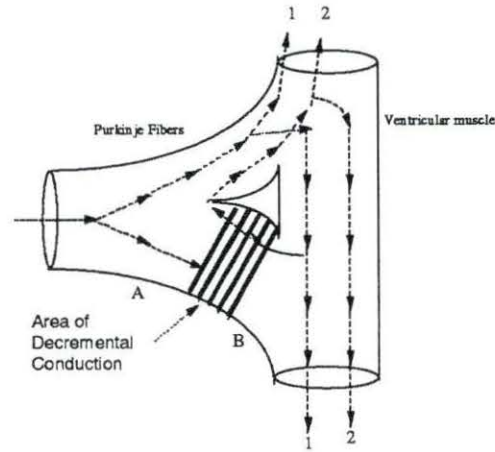
Figure 1.1:   The Infarcted Heart

## 1.7   Summary of Previous Work

Berbari [1] and Flowers [6] were the first to describe the anatomic basis for late
potentials.   Gardner [9] described in detail the electrophysiological basis for frac-
tionated electrocardiograms recorded from healed myocardial infarctions. The signal
characteristics at the tissue level were studied in this paper.  Simson [10] derived
the proper identification criteria and perfected the recording procedures.  This is
now the accepted technique for the identification of late potentials. Signal averaged
electrocardiograms were studied in detail by Sherif in [2]. Interest in beat-to- beat
detection was studied by Sherif and Mehra [11]. S. Jesus [12] described a Kalman
filter approach for this problem.  Simultaneously spatial averaging techniques for
beat-to-beat detection was proposed by Shelton [13]. The first known late potential
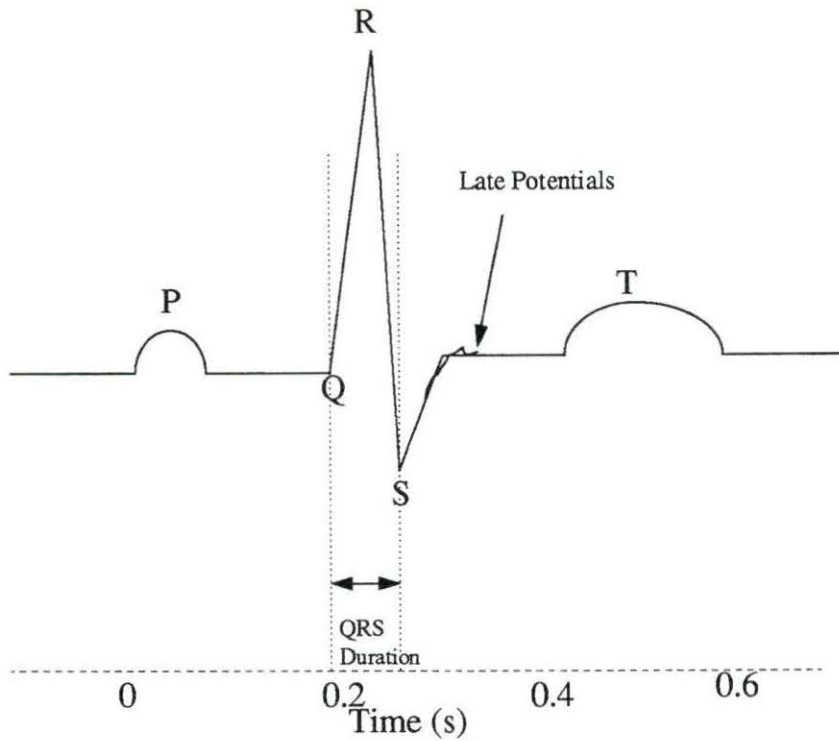
Figure 1.2: A Typical X Lead ECG Waveform

synthesis was done by Tuteur in [14]. Tuteur modeled late potentials as a sine wave modulated by a gaussian envelope and he applied wavelets transformations to detect these synthesized late potentials. Autoregressive modeling was done by Lander, et.al, [15] to detect intra-QRS late potentials. Spectrotemporal maps and frequency domain analysis using autoregressive modeling was perfected by Chan [16]. These methods are now applied real time in commercial devices to detect late potentials using spectrotemporal maps. Statistical methods like the maximum likelihood estimator were used to detect late potentials by Attarinejad [17]. Cameron,et.al, [8] suggested modeling of the late potentials as a decaying $sin(x)/x$ function and per-

formed bispectral analysis. Detection of a late potentials using adaptive filters was first suggested by Al-Nashash [18] and Wang [19]. Shelton and Coast also proposed detection of late potentials by adaptive filtering [20]. Recursive least squares filtering was suggested by Cameron [21] and the time variant filter was suggested by Coast [20]. Both [20, 21] showed results for synthesized late potential's. It was however observed that late potential's have not been modeled successfully in literature. The recent method for detection of late potentials was suggested by Chen [22] using Prony's method. Most researchers who applied different feature extraction techniques like wavelet transforms or Prony's method or other statistical estimators have used the averaged electrocardiogram. The question arises whether any variable late potentials have been lost.

## 1.8   Scope of This Thesis

The signal averaged ECG primarily uses two signal processing techniques to process the cardiac signal for late potential analysis: time ensemble averaging; and filtering. The standard technique for detection of VLP's results in a time-domain vector magnitude time series formed from a signal averaged, high pass filtered, three lead data set. The averaging technique can only detect late potentials which are absolutely constant in duration, morphology, and timing with respect to the QRS complex. Therefore, this technique cannot detect any beat-to-beat variations. Recording of late potentials on a beat-to-beat basis has the potential of directly identifying reentrant 'malignant' versus focal 'benign' ventricular rhythms [2, 23]. Researchers found that spatial averaging is an alternative to the time average. But spatial averaging is limited by the number of electrodes that can be placed on the chest. In this

thesis techniques to detect late potentials real time using adaptive filters is described. The leaky least means square algorithm was proposed as an alternative to the least mean square algorithm (LMS) as it yields a higher SNR. Dynamic time warping techniques were studied for coherent averaging of ECG signals. A statistical model was described for synthesizing late potentials and the time sequenced adaptive filter was modified to yield a higher SNR and this can be used as a better technique to detect late potentials on a beat-to-beat basis. Time varying filters are also described as a method to improve the SNR and detect time varying late potentials.

# CHAPTER 2.   HIGH RESOLUTION ELECTROCARDIOGRAPHY

## 2.1   Introduction

Ambulatory electrocardiography is recognized as a valuable non-invasive cardio-logic diagnostic test to asses changes of cardiac arrhythmias and heart rate variability [11]. It has been observed that this scheme is not suitable to detect high frequency cardiac depolarizations. High resolution electrocardiography is the technique that is used to enhance the detection of low amplitude signals. The hardware used in this technique is described in the following section. The signal averaged ECG system is shown below in Figure 2.2.

## 2.2   Technical Aspects of Signal Averaged ECG System

The standards for the hardware are defined in [24]. Commercially available devices comply with this standard.

### 2.2.1   Electrodes

Real-time signal averaging utilizes three orthogonal bipolar leads $X$ $Y$ and $Z$ to record the cardiac electrical activity from the body surface. For recording late potentials from the surface of the body, most investigators use an $XYZ$ lead system formed by three orthogonal bipolar electrode combinations (see Figure 2.1). The
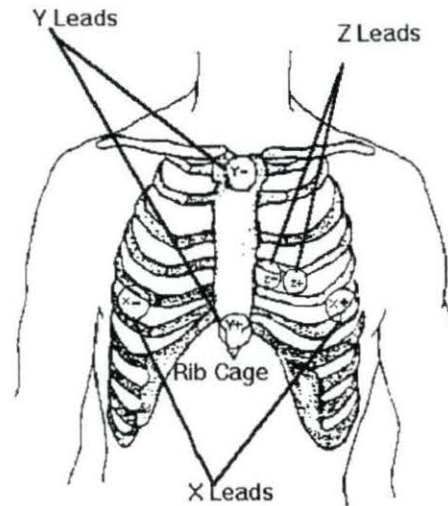
Figure 2.1:   XYZ Electrode Placement Scheme

$X$ lead is placed at the fourth intercostal space in both midaxillary lines. The $Y$ lead should be positioned on the superior aspect of the manubrium and on either the upper left leg or left iliac crest. The $Z$ lead should be positioned at the fourth intercostal space ($V_2$) position . Silver-silver chloride electrodes are used and the skin impedance should be less than 1000$\Omega$.

### 2.2.2   Hardware

The typical hardware is shown in Figure 2.2. The ECG signal obtained from the orthogonal leads is amplified and the data is sampled at 1000 Hz. The A/D converter has a 12 bit precision. The software performs three functions; detection, template

## Signal Averaging Technique
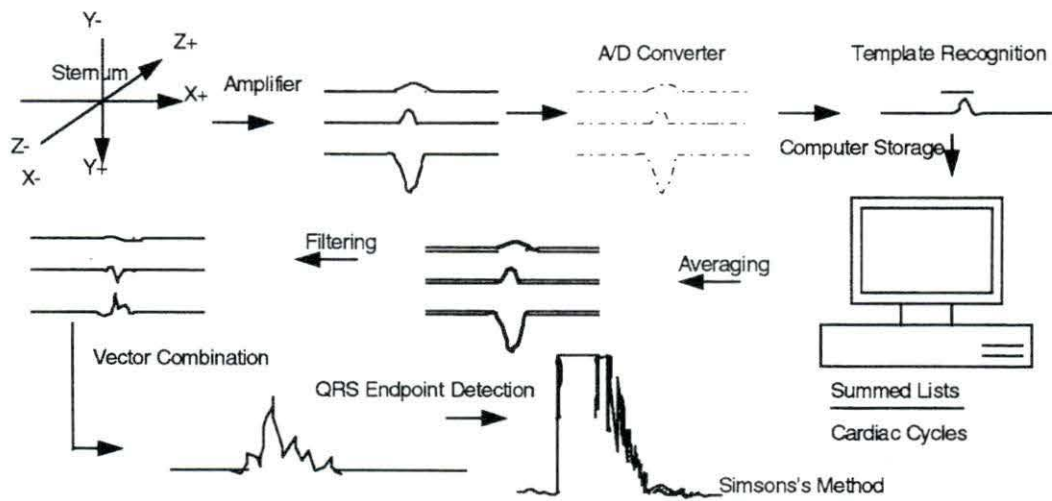


Figure 2.2: The Signal Average ECG System

matching and alignment of the accepted QRS complexes. Time domain analysis is done using the Simson's method. The beats after alignment and summation are passed through a bi-directional four pole Butterworth filter as recommended by the American College of Cardiology (ACC) policy statement [24]. Ringing effects of high pass filtering may prevent proper quantification of late potentials. Simson [4] adopted a variant of bi-directional filtering. The data is filtered roughly until the mid point of the QRS and then stops filtering which allows the ringing to subside before the end of the unfiltered QRS. The data is then reverse filtered through the same point until the QRS mid point. The filter has a bandpass 40-250 Hz or 20-250 Hz. Results are based on analysis of the vector magnitude of the filtered leads that is known as the RMS value and is defined $\sqrt{X^2 + Y^2 + Z^2}$. The endpoint and onset of the filtered QRS duration is then verified visually by the technician.

## 2.3   Signal Averaging

These standards indicate that the noise should be less than $1mV$ with a 25 Hz high pass or less than $0.7\mu V$ with a 40 Hz cut off when used with the combined vector magnitude of $XYZ$ leads. The first step is to find a reference point. For this purpose the $R$ wave is usually selected. After this, beats are aligned and averaged. The computer algorithm should be capable of excluding ectopic (noisy) beats. Testing of new beats should be performed across all input leads. Mostly a cross-correlation is used for template matching and a correlation greater than 98% is used for acceptance. Beats are accepted for averaging only if the $R$ wave to $R$ wave is within 20% of the previous R-R interval.

## 2.3.1 Time Domain Analysis

Results of most studies have been based on the analysis of the vector magnitude of the filtered QRS complex. The filtered QRS duration, RMS amplitude of the terminal $40msec$ of the QRS complex, and the low amplitude signal duration measured from the QRS endpoint until the signal exceeds $40\mu V$ are the parameters needed to establish the presence of fragmented potentials (Figure 2.3). The filtered QRS complex is defined as the midpoint of a $5msec$ segment in which the mean voltage exceeds the mean noise level plus three times the standard deviation of the noise sample [2]. The endpoint of the QRS complex should be verified visually and the system allows manual adjustment of the automatically determined end points. The definition of a late potential and the scoring of a high resolution ECG as normal or abnormal have not yet been standardized [24]. Representative criteria include that a late potential exists (using 40 Hz high pass bi-directional filtering) when

1. The filtered duration of the QRS complex is greater than $114msec$.

2. There is less than $20\mu V$ of signal in the last $40msec$ of the vector magnitude complex, and

3. The terminal vector magnitude complex remains below $40\mu V$ for more than $38msec$.
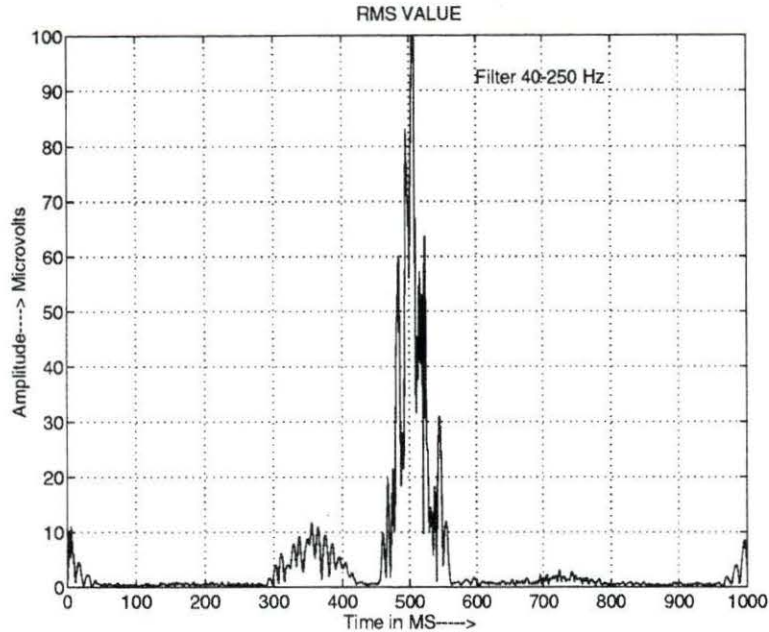
Figure 2.3:   Root Mean Square Value

## 2.4   Beat to Beat Analysis of ECG signals

### 2.4.1   Disadvantages of the Signal Averaged ECG System

Signal averaging techniques has many disadvantages. The two major limitations are that it will not be able to detect dynamic (beat-to-beat) changes in the signal due to sinusrhythm; and the SAECG cannot be recorded during complex cardiac arrhythmias. The variability of the R-R intervals is seen in Figure 2.4. The QRS detection algorithms [25] perform poorly under low SNR conditions. This is demonstrated in Figure 2.4. The first graph shows the QRS detection algorithm [26] in a
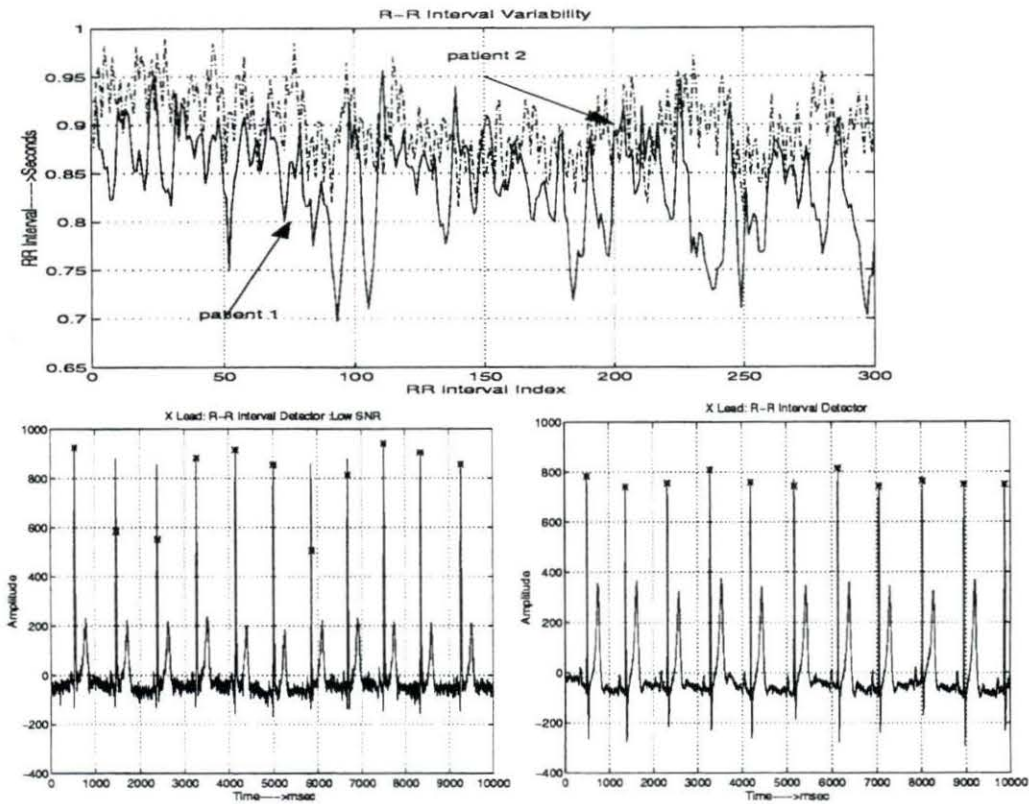
Figure 2.4: RR Interval Variability and RR Detection

low SNR environment and the other shows the performance of the algorithm under a high SNR. Even $\pm 3msec$ error in detection of peaks may cause a significant change in the quantification of late potentials.

Each of these problems are addressed separately. As described in Chapter 1, the statistical properties of the late potentials has not been well documented. But due to the variable nature of the heart's oscillator, it is believed that the late potentials may exhibit cyclostationary properties. That is, the statistics of the signal may be repeated in multiple periodicities [21]. The detection of time varying signals is beyond the scope of the averaging technique. The signal averaging technique is done under

the assumption that the late potentials are constant in timing relative to the QRS. Another assumption is that the late potentials are fixed in both morphology and duration. These are poor assumptions as the late potentials are influenced by factors like the nature of the infarct and the time or the number of days after the infarct [6]. Since late potentials originate from ischemic areas where physiologic conditions are unstable, they are inherently variable in terms of amplitude, bandwidth, and timing within the cardiac cycle [23]. The variability of late potentials are compounded by variations in the heart rate in Figure 2.4. Variations in heart rate as small as 20% can shift the activation patterns on ischemic ventricles by as much as $10msec$. The results obtained from signal averaging also depend on the alignment of the beats. The QRS detectors have to be very precise else the QRS may manifest as a late potential. Probably the most important and best known source of beat-to-beat variability in cardiac electrical signals is respiration. Expansion of the thorax during inspiration produces two effects on the ECG. First, it induces a direct baseline shift mainly as a result of electrode impedance change and, second, it alters the electrical propagation of electrical signals from the heart to the body surface. Both artifacts can introduce significant timing errors and need to be considered. A study [23] showed that the most prominent influence on the orthogonal leads were on the QRS amplitude and azimuth. During deep inspiration, the QRS amplitude declined by 25% and azimuth increased significantly (in 69 patients) by an average of 11°. Respiration thus adversely influences the ability to align successive QRS complexes and determine the fiducial points. The effect of respiration was shown by simulating the ECG with a sinusoidal equation [23].

$$y(t) = asin(2\Pi/T + \Phi - sin(\Phi))$$
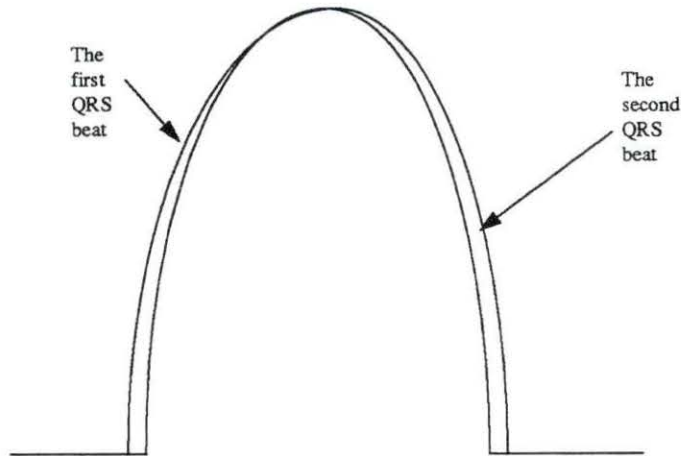
Figure 2.5:   The Differences in Two QRS Beats

Two QRS beats are shown above in Figure 2.5. As can be seen, perfect alignment of these complexes is not possible and hence any method including cross correlation will accumulate errors.

## 2.4.2   Statistics of the ECG Signal

The ECG signal contains noise components that can be traced to patient related origins, e.g., muscular activity and to the electronics of the recording equipment. Knowledge of the statistics of the noise is important to calculate the QRS endpoints in the Simson's method. Besides quantization noise, the four primary sources of noise

are power frequency, electrode-skin interface, amplifier noise and electromyogram (EMG) signals. The noise is assumed to be uncorrelated with the ECG. However low frequency noise due to respiration may have a beat-to-beat correlation, which is removed by high pass filtering [18].

### 2.4.3 Methods of Noise Reduction

1. Signal Averaging

Signal averaging is analogous to low pass filtering. The signal averager may be viewed as a comb filter. The improvement in signal to noise ratio (SNR: defined as the ratio of the signal power to the noise power) varies as $\sqrt{N}$ where $N$ is the number of averages. Consider adding together $N$ beats and forming a mean beat or signal average $\hat{x}(i)$. This is given as

$$\hat{x}(i) = \frac{\sum\limits_{j=1}^{N} x_j(i)}{N} \tag{2.1}$$

where $x_j(i)$ is beat $j$ in $N$ $^{th}$ beat ensemble. The addition of the signal and noise components can thought of as taking place independently that is

$$\hat{x}(i) = \frac{\sum\limits_{j=1}^{N} s_j(i)}{N} + \frac{\sum\limits_{j=1}^{N} n_j(i)}{N} \tag{2.2}$$

Since the cardiac signal is assumed to be identical, $\sum\limits_{j=1}^{N} s_j(i)/N = s(i)$. The summation of noise proceeds in from three assumptions. The noise is assumed to be zero mean. The noise is a random process uncorrelated with the cardiac signal and is considered across the ensemble. The noise occurring at the same time may be considered to be independently and identically distributed. Then

$$\sum_{j=1}^{N} n_j(i) = \frac{\hat{n}(i)}{\sqrt{N}} \tag{2.3}$$

hence the signal average is

$$\hat{x}(i) = s(i) + \frac{\hat{n}(i)}{\sqrt{N}} \tag{2.4}$$

2. Ensemble Averaging

Researchers studied spatial averaging as a method to improve the SNR [13]. Significant improvement in the SNR was observed in comparison with the signal averaging technique. The major advantage of spatial averaging is that it allows appreciation on a beat-to-beat basis of changing R-R intervals and other dynamic changes in the heart. As spatial averaging requires averaging only two channels, the noise level in the vector magnitude was still high. There are many limitations to the spatial averaging technique. This technique is limited by the number of leads that can be placed on the chest. It is difficult to find a good lead position. The EMG noise in the parallel channels is not completely uncorrelated with each other and it is difficult to determine what the best positions are for the placement of the electrodes.

### 2.4.4 Quantification of Noise

The literature shows inconsistencies for quantification of noise. The definition used in this work is adapted from [2] and [23]. The noise measure is calculated by selecting a signal free portion of the ECG signal that is in the later portion of the ST segment, in the $XYZ$ leads. The statistics of the noise was evaluated by calculating the histograms for samples in the ST segment (from the ST segment junction and

$100msec$ afterwards). It was observed that histograms closely approximate a gaussian distribution with a zero mean and a standard deviation between $10 - 20\mu Volts$. Simulations were carried out for different sets of ECG signals and for different leads. The mean value was subtracted in order to reduce the effect of the signal component when calculating the amplitude histograms. This technique was adapted from [27]. The assumption that the noise is gaussian is valid and the noise figure is calculated with those assumptions. A range of time windows for calculating the noise figure (N.F) was seen in the literature [23]. Noise in the three leads have different variances and closely approximate a gaussian distribution. Hence the vector magnitude is the sum of three non-central chi square distributions, resulting from the absolute value operation performed on each lead. The N.F suggested in the literature for a good estimate [23] is defined as

$$NF = \sqrt{\frac{1}{3m} \sum_{j=1}^{3} \sum_{k=1}^{m} \sigma_{Njk}^2} \qquad (2.5)$$

where $j$ indicates the lead $X, Y, Z$ and $m$ equals the number of points in each lead from which the noise is calculated. The N.F given in (2.5) is the average of the signal variance for $m$ points in the noise window which is again averaged over the three leads.

The square root of N.F is the standard deviation of the noise process. Dividing the N.F by $\sqrt{n}$ results in an average measure of the standard deviation. The reduction of the noise is observed in Figure 2.6 as a function of the number of averages. A $10msec$ window was used to estimate N.F. For a variety of reasons, some ECG signals have a poor SNR and the burst of noise observed in the ECG signal is due to muscle movement. Such bursts can be detected in the noise curve and is used as a control
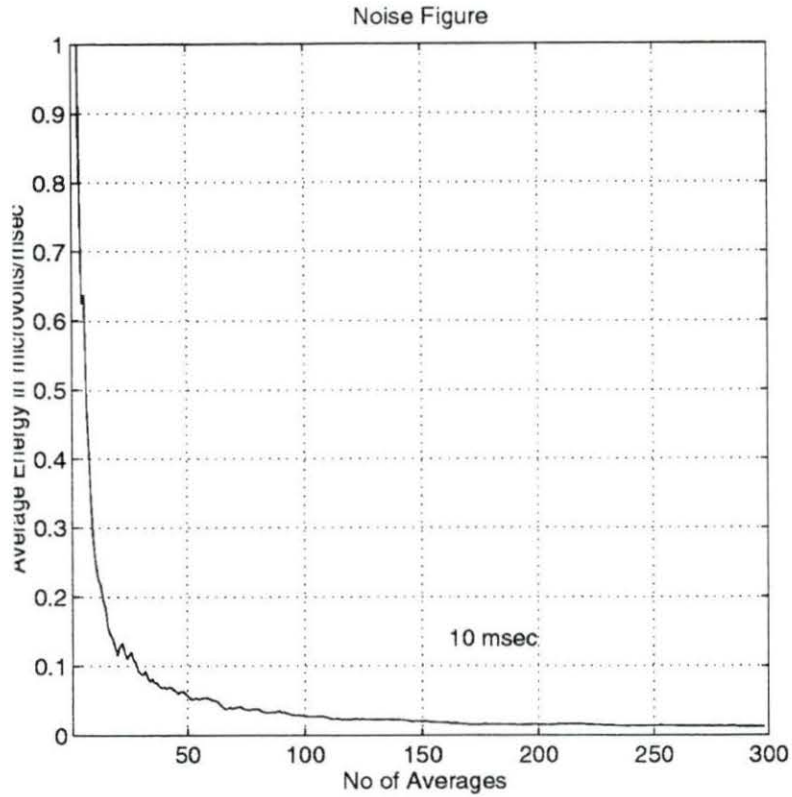
Figure 2.6: Calculation of Noise Figure

measure. Averaging to a noise factor of $< 0.3\mu V$ is required for the accurate detection of late potentials.

## 2.5    Proposed System

This thesis studies the different beat-to-beat techniques that can be applied to detect late potentials and study their nature from beat-to-beat. This thesis presents a real time system to detect the late potentials on a beat-to-beat basis. Beat-to-beat detection can be achieved only if the signal has a high SNR on individual beats. The

DSP 56001
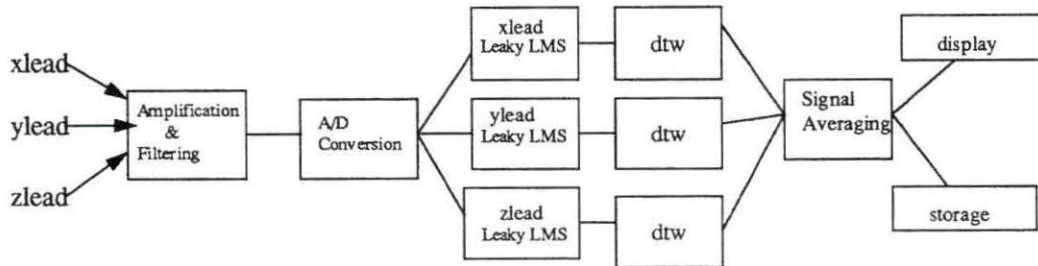


Figure 2.7:   Proposed Real Time System

commercial devices that exists run on the Motorola 68K processor working as fast as 27K instructions per second. Thus this system is limited in speed. The commercially available SAECG devices average anywhere between 250-300 cycles to reduce the noise to approximately $< 0.3\mu Volts$. Thus at a sampling rate of 1000 Hz and each QRS beat almost a second this corresponds to 4-5 minutes before the RMS values can be determined. The Leaky LMS algorithm is used for the enhancement of late potentials. The Motorola 56K processor can be used to run this algorithm. It works at a speed of 13.5 million instructions per second. Approximately 13,000 instructions can be performed at a rate of one sample per millisecond. Thus cross-correlation, Butterworth filtering, LMS and the RMS (for detection of late potentials) calculation can be performed between beats. The DSP based SAECG algorithm can be used to generate the RMS value in seconds and is easily incorporated into a stand alone system. The LMS algorithm is run in a simulator to test the results. The system block diagram is shown in Figure 2.7.

Dynamic time warping is a technique used to align speech signals which differ due to speaking rate variation. This technique is used if time averaging of the beats is needed when the SNR from beat-to-beat is low. This is done to achieve a coherent averaging scheme. Noise figures in the latter $10 - 110msec$ of the ST segments were calculated and a comparison was made with the existing averaging techniques. The results show that the adaptive filtering enhancement of the low level cardiac signals on a beat-to-beat basis is significant. Other techniques like least squares filtering and time varying filters were also studied. The results are shown in Chapter 6.

# CHAPTER 3.  ADAPTIVE NOISE CANCELER

## 3.1  Introduction

The usual method of estimating a signal corrupted by additive noise is to pass the composite signal through a filter that tends to suppress the noise while leaving the signal relatively unchanged. Filters used for this purpose can be fixed or adaptive. The design of fixed filters must be based on priori knowledge of both the signal and the noise, but adaptive filters have the ability to adjust their own parameters automatically, and their design requires little or no prior knowledge of signal and noise characteristics. Noise cancellation is a variation of optimal filtering that is highly advantageous in many applications. It uses an auxiliary or reference input containing both signal and noise. As a result, the primary noise is attenuated or eliminated by cancellation. Adaptive noise cancellation was successfully applied to cancelling 60 Hz noise in electrocardiography by Huhta and Webster [27] and by Widrow to cancel the donor heart interference in heart transplant electrocardiography. Widrow [27] also applied this principle to cancel the maternal ECG in fetal electrocardiography.

## 3.2  Principle of a Correlator Canceler

A correlator canceler is the best linear processor for estimating one signal from another in terms of minimizing the mean square error. It is a precursor to Wiener
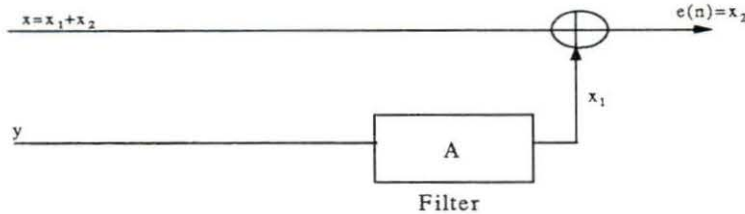
Figure 3.1: Correlator Canceler

filtering. Figure 3.1 illustrates the basic principle of a correlator canceler. If $x$ has a part $x_1$ which is correlated with $y$. Then $x_1$ is will be canceled as much as possible from the output so as to minimize the mean square error. The correlator canceler is the optimal estimate of $x$ from $y$. It can be viewed as an optimal signal separator that cancels that portion of $x$ which is correlated with $y$. The adaptive noise canceler is based on the principle of a correlator.

The basic noise canceling situation is illustrated in Figure 3.2. A signal is transmitted over a channel to a sensor that receives the signal plus an uncorrelated noise $v(n)$. The combined signal and noise $x(n) + v(n)$ forms the primary input to the canceler. A second sensor receives a signal and uncorrelated noise that is $y(n)$. This sensor provides the reference input to the canceler. The noise $v(n)$ is filtered to produce an output $d(n)$ that is a close replica of $x(n)$. If one knew the characteristics of the channels over which the noise was transmitted to the primary and reference sensors, one could in general design a fixed filter. Noise free output from a fixed filter is difficult to achieve. The characteristics of the transmission paths are assumed to be unknown or known approximately, and the use of fixed filter is not feasible. The
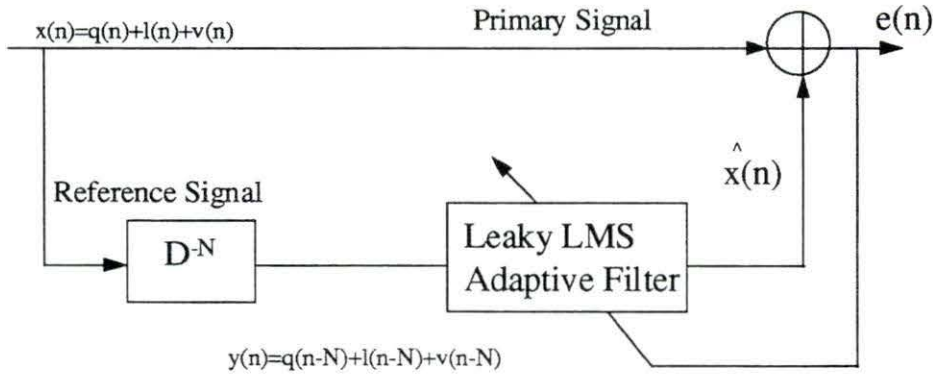
Figure 3.2: The Leaky LMS

characteristics of the ideal fixed filter would have to be adjusted with a precision difficult to attain, and the slightest error could result in increased noise at the output. In the system shown in Figure 3.2 a slight modification of the above scheme is used. The reference input is derived from the primary input. The reference is delayed by $N$ samples. The value of $N$ was found by empirical methods. From the principle of the correlator canceler, it is known that for Figure 3.2

$$R_{ey} = E\left[ey^H\right] \tag{3.1}$$

where $R$ is the cross correlation matrix, $e$ is the error signal $y$ is the output.

$$R_{ey} = E\left[(x - Ay)\, y^H\right] \tag{3.2}$$

hence solving (3.2) we get

$$A = R_{yy}^{-1} R_{xy} \tag{3.3}$$

Let $x$ be composed of the following

$$x(n) = q(n) + l(n) + v(n) \tag{3.4}$$

Where $q(n)$ is the ECG signal which is observed from beat-to-beat. $l(n)$ is the late potential which is also observed from beat-to-beat and $v(n)$ is the white noise. Let $y(n)$ consist of the following signals i.e.,

$$
\begin{aligned}
y(n) &= q'(n) + l'(n) + v'(n) \\
y(n) &= q(n-N) + l(n-N) + v(n-N)
\end{aligned}
\tag{3.5}
$$

$y(n)$ is derived by delaying $x(n)$ by $N$ samples. Hence (3.2) becomes

$$E\left(ey^H\right) = E\left((q+l+v) - A\left(q'+l'+v'\right)y^H\right) \tag{3.6}$$

The assumption made is that $E[vv'] = 0$ after the data is shifted by $N$ samples and that $E[qq']$ and $E[ll']$ are non zero after a delay of $N$ samples. Hence from (3.3) and (3.6). we can show that

$$\hat{x} = R_{ss} R_{yy}^{-1} y \tag{3.7}$$

where $s(n) = l(n) + q(n)$.

In practice we assume that the autocorrelation of the white noise is not significant after about 50 samples. The signals are strongly correlated within this lag. Any gradient descent algorithm can be used to reach this optimum Wiener solution. The Leaky LMS algorithm is discussed below.

## 3.3   LMS and the Leaky LMS

The mean square error performance surface for the adaptive system is a quadratic function of the weights when the input and the desired response are statistically stationary. The task is to seek the minimum point on the performance surface. The LMS algorithm uses a special estimate of the gradient. The LMS algorithm is important because of its simplicity, ease of computation and because it does not require off-line gradient estimations or repetitions of data. The Leaky LMS is a variant of this algorithm. An equivalent leaky LMS can be realized by adding white noise of mean zero and variance $\alpha$ to the tap-input vector of the conventional LMS algorithm. The time varying cost function is defined as follows

$$J(n) = |e(n)|^2 + \alpha \|w(n)\|^2 \qquad (3.8)$$

where $w(n)$ is the tap weight vector of the transversal filter, $e(n)$ is the estimation error and $\alpha$ is a constant. The error surface can be rewritten as

$$J(w) = \sigma_d^2 - w^H P - P^H w + w^H R w + \alpha w^H w \qquad (3.9)$$

The gradient is given by the derivative

$$\frac{\partial J}{\partial w^*} = -P + Rw + \alpha w \tag{3.10}$$

Hence the recursive equation to calculate the weights can be easily derived as

$$\hat{w}(n+1) = \hat{w}(n) - \mu \frac{\partial J}{\partial w^*} \tag{3.11}$$

Hence we can derive the update equation as follows

$$\hat{w}(n+1) = (1 - \mu\alpha)\hat{w}(n) + \mu U(n)e^*(n) \tag{3.12}$$

Where $0 \leq \alpha \leq \frac{1}{1-\mu}$

The Wiener solution can also be derived by taking the expectations on both sides of (3.12) and its given as follows

$$E\left[\hat{w}(n)\right]_{n \longrightarrow \infty} = (R + \alpha I)^{-1} P$$

# CHAPTER 4. DYNAMIC TIME WARPING

## 4.1 Introduction

Ventricular late potentials are time varying signals. Coherent averaging of these signals can be achieved if this fluctuation in time is avoided. Linear time normalization techniques are insufficient to deal with highly non-linear fluctuation. The dynamic programming - matching technique was studied by Sakoe and Chiba for speech recognition [28]. It is well known that speaking rate variation causes nonlinear fluctuation in a speech pattern time axis. Elimination of this fluctuation is called time normalization. The time-axis fluctuation is approximately modeled with a nonlinear warping function with some carefully specified properties. Timing differences between two speech patterns are eliminated by warping the time axis of one to the that of the other. Then the time normalized distance is calculated as the minimized residual distance between them. This minimization process is very efficiently carried out by use of dynamic programming. This technique is used to obtain a coherent time averaging scheme with ECG signals in this thesis. An optimum algorithm for dynamic programming matching is shown in [28]. There are two kinds of dynamic programming algorithms, the symmetric and asymmetric algorithm. In the asymmetric form, time normalization was achieved by transforming the time axis of one pattern onto that of the other. In the symmetric form, both axes are transformed into
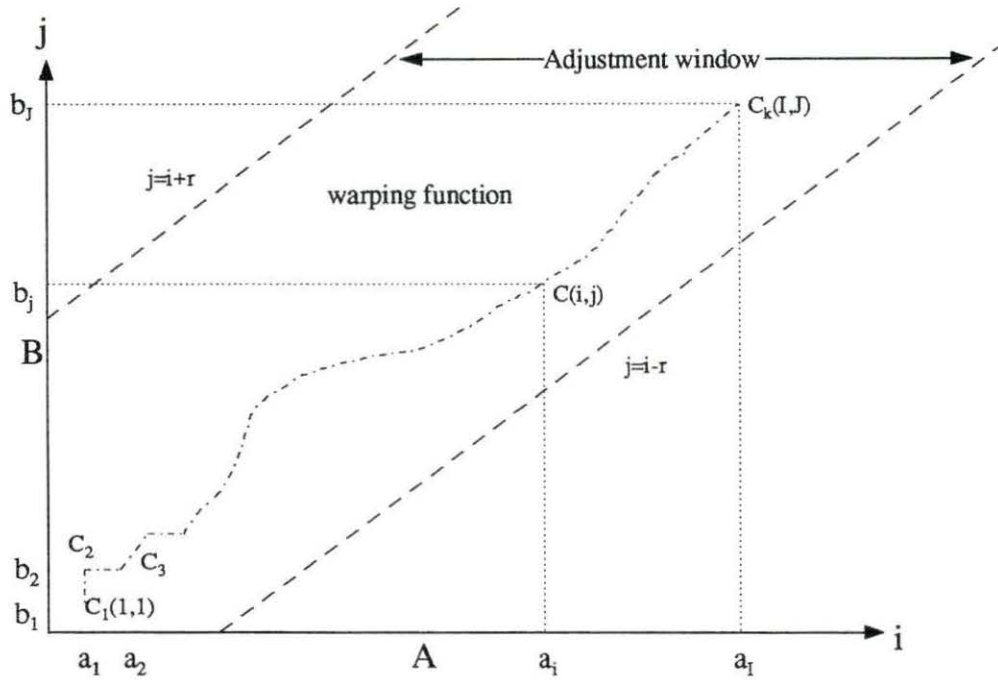
Figure 4.1:   The Warping Function

a temporarily defined common axis. A slope constraint is introduced. This is done so that the flexibility of the warping function is restricted. If the warping function is very flexible then it may result in poor warping. This problem is discussed in a later section.

## 4.2 Warping Principle

The signal can be expressed by appropriate feature extraction as a sequence of feature vectors.

$$A = a_1, a_2, \ldots a_i, \ldots, a_I \tag{4.1}$$
$$B = b_1, b_2, \ldots b_j, \ldots, b_J$$

Consider the problem of eliminating the timing differences between those two patterns. In order to clarify the nature of time-axis fluctuation or timing differences, let us consider an $i - j$ plane as shown in Figure 4.1 where $A$ and $B$ are developed along the $i-$ axis and $j-$ axis respectively. Where these signal patterns are of the same category, the timing differences between them can be depicted by a sequence of points $c = (i, j)$.

$$F = c(1), c(2), \ldots c(k), \ldots c(K) \tag{4.2}$$

where

$$c(k) = (i(k), j(k)) \tag{4.3}$$

This sequence can be considered to represent a function which approximately realizes a mapping from the time axis of pattern $A$ onto that of $B$. It is called a warping function. When there is no timing difference between these patterns, the warping function coincides with the diagonal $j = i$. It deviates further from the diagonal line as the timing difference grows. As a measure of the difference between the elements of the feature vectors, i.e., $a_i$ and $b_j$ is a distance defined by

$$d(c) = d(i, j) = |a_i - b_j| \tag{4.4}$$

Then the weighted summation of distances on the warping function $F$ becomes

$$E(F) = \sum_{k=1}^{K} d(c(k)) w(k) \tag{4.5}$$

(where $w(k)$ is a non-negative weighting coefficient, which is intentionally introduced to allow the $E(F)$ measure, a flexible characteristic) and is a reasonable measure for the goodness of the warping function $F$. It attains its minimum value when a warping function $F$ is determined so as to optimally adjust the timing difference. This minimum residual distance value can be considered to be a distance (between patterns $A$ and $B$) still remaining after eliminating the timing differences between them, and is naturally expected to be stable against time-axis fluctuation. Based on these considerations, the normalized distance between two signal patterns $A$ and $B$ is defined as follows:

$$D(A, B) = \left[ \frac{\sum_{k=1}^{K} d(c(k)) w(k)}{\sum_{k=1}^{K} w(k)} \right] \tag{4.6}$$

where the denominator is employed to compensate for the effect of $K$ (number of points on the warping function $F$). (4.6) is no more than a fundamental definition of time normalized distance. Effective characteristics of this measure greatly depend on the warping function specification and the weighting coefficient definition. Desirable characteristics will vary according to the signal pattern properties (especially time axis expression of speech pattern) to be dealt with.

## 4.2.1 Restrictions of the Warping Function

The warping function $F$, defined by (4.6) is a model of the time-axis fluctuation in a given pattern. Accordingly, it should approximate the properties of actual time-axis fluctuation. In other words, function $F$, must preserve essential structures in pattern $A$ and vice versa. Essential speech pattern time axis structures are continuity, monotonicity, slope limitation and so on. These considerations can be realized by the following restrictions on the warping function $F$ (or points $c(k) = (i(k), j(k))$).

1. Monotonic conditions

$$i(k-1) \le i(k) \text{ and } j(k-1) \le j(k)$$

2. Continuity conditions

$$i(k-1) - i(k) \le 1 \text{ and } j(k-1) - j(k) \le 1$$

As a result of the two restrictions the following relation holds between two consecutive points.

$$c(k-1) = \begin{cases} (i(k), j(k)-1) \\ (i(k)-1, j(k)-1) \\ (i(k)-1, j(k)) \end{cases}$$

3. Boundary conditions

$$I(1) = 1, j(1) = 1 \text{ and } I(K) = I, J(K) = J$$

4. Adjustment window condition Figure 4.1

$$|i(k) - j(k)| \le R$$

where $r$ is an appropriate positive integer called window length. This condition corresponds to the fact that time-axis fluctuation in usual cases never causes an excessive timing difference.

5. Slope constraint condition

Neither too steep nor too gentle a gradient should be allowed for warping function $F$ because such deviations may cause undesirable time-axis warping. A very steep gradient, for example, causes an unrealistic correspondence between a very short pattern $A$ and a relatively long pattern $B$ segment. Therefore a restriction called a slope constraint condition, was set upon the warping function $F$. This is shown in Figure 4.2. If the point $c(k)$ moves forward in the direction of $I$ (or $J$) axis consecutive $m$ times, then the point $c(k)$ is not allowed to step further in the same direction before stepping at least $n$ times in the diagonal direction. The effective intensity of the slope constraint can be evaluated by the following measure $P = n/m$.

The larger the $P$ measure, the more rigidly the warping function slope is restricted. When $P = 0$, there are no restrictions in the warping function. When $P = \infty$ (that is $m = 0$), the warping function is restricted to diagonal $j - i$. Nothing more occurs than a conventional pattern matching; no time normalization. Generally speaking, if the slope constraint is too severe, then time-normalization would not work effectively. If the slope constraint is too lax, then discrimination between signal patterns in different categories is degraded. Thus, setting neither a too large nor a too small slope for $P$ is desirable.
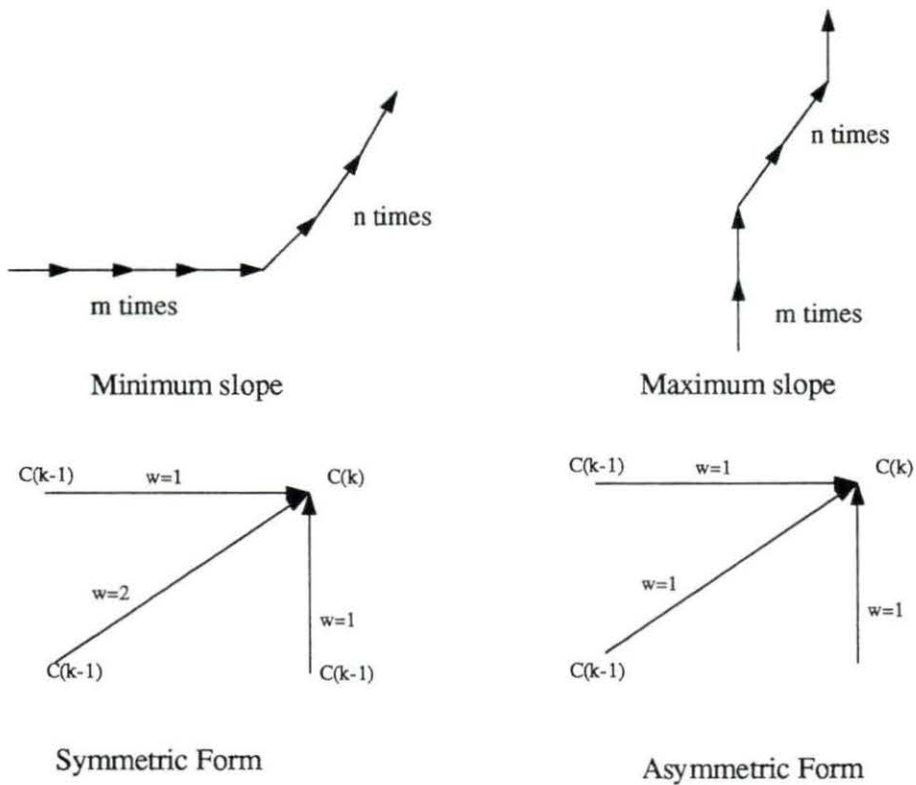
Figure 4.2: The Different Warping Algorithms

## 4.2.2 Weighting coefficient

If the denominator in (4.6) called the normalization coefficient is independent of the warping function $F$, this simplifies the equation as follows:

$$D\left(A,B\right) = \frac{1}{N}\min_{F}\left[\sum_{k=1}^{K}d\left(c\left(k\right)\right)w\left(k\right)\right]$$

$$N = \sum_{k=1}^{K}w(k)$$

(4.7)

This simplified problem can be effectively solved by use of the dynamic programming technique. There are two typical weighting coefficient definitions which enable this simplification. The theory is described as follows:

1. Symmetric form:

$$w(k) = (i(k) - i(k - 1) + j(k) - j(k - 1))$$

then $N = I + J$ where $I$ and $J$ are the length of the patterns $A$ and $B$ respectively.

2. Asymmetric form:

$$w(k) = (i(k) - i(k - 1))$$

then $N = I$. The basic concepts of the symmetric and asymmetric forms were originally defined by Sakoe and Chiba [28].

## 4.3  Practical DP matching Algorithm

### 4.3.1  DP equation

A simplified definition of time-normalized distance $D(A, B)$ as given by (4.7) is one of the typical problems to which the well known DP-principle can be applied. The basic algorithm for calculating (4.7) is written as follows.
Initial condition

$$g_1(c(1)) = d(c(1))w(1)$$

DP equation:

$$g_k(c(k)) = \min_{c(k-1)}[g_{k-1}(c(k - 1)) + d(c(k))w(k) \tag{4.8}$$

Time normalized distance:

$$D(A, B) = \frac{1}{N} g_k c(K)$$

It is implicitly assumed that $c(0) = (0,0)$. Accordingly $w(1) = 2$ in the symmetric form, and $w(1) = 1$ in the asymmetric form. The restriction on the warping function is realized by incorporating the weighting coefficient $w(k)$. The algorithm for the symmetric form in which no slope constraint is employed is described in (4.9). The initial condition is given by

$$g(1, 1) = d(1, 1)$$

D.P. equation:

$$g(i, j) = \min \begin{bmatrix} g(i, j - 1) + d(i, j) \\ g(i - 1, j - 1) + d(i, j) \\ g(i - 1) + d(i, j) \end{bmatrix} \qquad (4.9)$$

The restriction condition (adjustment window)

$$j - r \le i \le j + r$$

Time normalized distance:

$$\begin{aligned} D(A, B) &= \frac{1}{N} g(I, J) \\ \text{where } N &= I + J \end{aligned}$$

The algorithm, especially the DP equation, should be modified when the asymmetric form is adopted or some slope constraint is employed. Chiba [28] summarizes algorithms for symmetric and asymmetric forms. A flow chart is given in Figure 4.3 which describes the algorithm.

### 4.3.2 Calculation

DP equation of $g(i, j)$ must be recurrently calculated in ascending order with respect to coordinates $I$ and $J$, starting from initial condition at $(1, 1)$ up to $(I, J)$. The domain in which the DP equation must be calculated is specified by

$$1 \leq i \leq I$$
$$1 \leq j \leq J \text{ and}$$

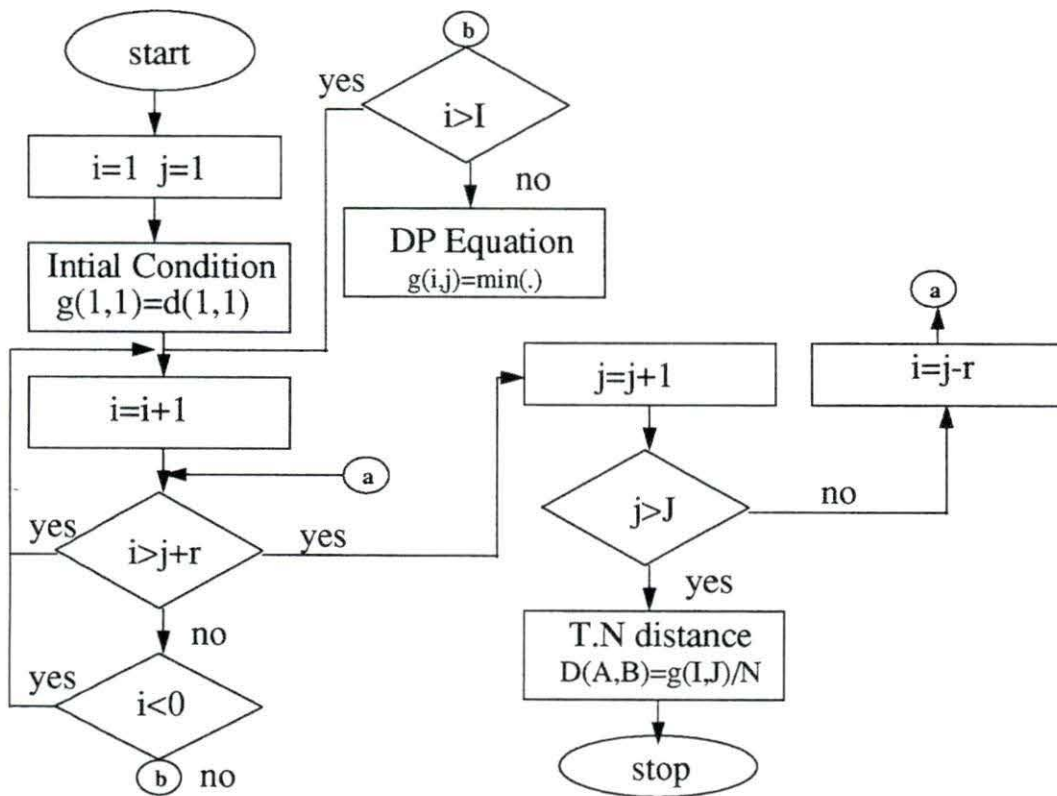$$j - r \leq i \leq j + r$$

and $r$ is the adjustment window.

41



Figure 4.3:  Flow Chart for DTW

## CHAPTER 5.   TIME - SEQUENCED ADAPTIVE FILTER

### 5.1   Introduction

Late potentials are time varying signals and the location of this time varying signal can be identified as $150msec$ after the occurrence of the $R$ wave in the ECG waveform. Therefore a time varying filter will be able to catch the variations of the late potentials on a beat-to-beat basis. A new form of adaptive filter was proposed by Ferrara and Widrow [29] which will be used for the estimation of a class of non-stationary signals. This new filter, called the time sequenced adaptive filter is an extension of the LMS adaptive filter. Both the LMS and the TSAF are digital filters composed of a tapped delay line, whose impulse response is controlled by an adaptive system. For stationary stochastic inputs, the mean- square error, which is the expected value of the squared distance between the filter output and externally supplied desired response, is a quadratic function of the weights. This is a paraboloid with a single fixed minimum point which can be sought by gradient techniques like the LMS. For non-stationary inputs however, the minimum point, curvature, and orientation of the error surface could be changing over time. The TSAF uses multiple sets of adjustable weights. At each point in time, one and only one set of weights is selected from the filter and is adapted using the LMS. The index set of weights that are chosen is synchronized with the recurring statistical character of the filter input
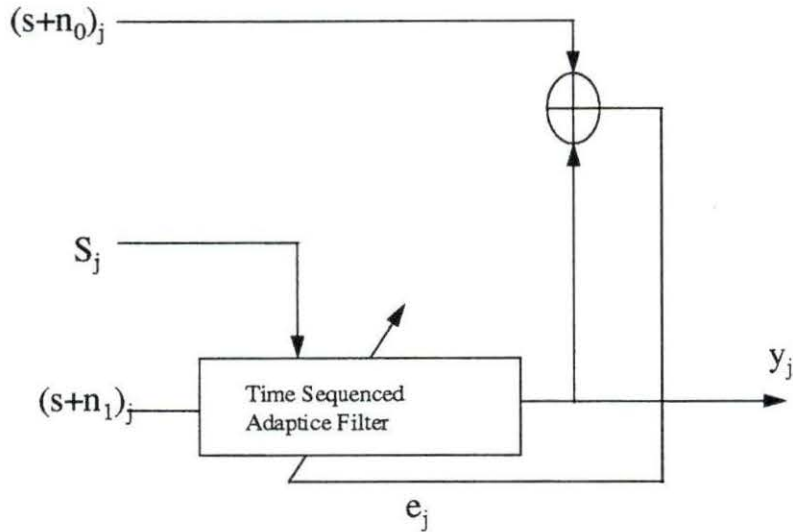
Figure 5.1:  Symbolic Representation

so that each set of weights is associated with a single error surface. After a number of adaptations of the weights, the minimum point of each error surface is reached resulting in a time-varying filter. For this filter, some apriori knowledge of the input is assumed. For pulse type signals, this could be the location of the pulses in time. For signals with periodic statistics, knowledge of the period is sufficient. This method was used to enhance fetal electrocardiograms against background muscle noise [30].

## 5.2   TSAF algorithm

An adaptive transversal filter consists of a tapped delay line connected to an adaptive linear combiner that adjusts the weights of the signals derived from the taps of the delay line and combines them to form an output signal. The input signal

vector $X_j$ of the adaptive linear combiner is defined as

$$X_j^T = \left[ x_j x_{j-1} ... x_{j-(n-1)} \right]^T \tag{5.1}$$

The input signal components are assumed to appear simultaneously on all input lines at discrete times indexed by the subscript $j$. The weighing coefficients or multiplying factors $w_0, w_1, w_2...w_n$. are adjustable. The weight vector $W$ is

$$W^T = [w_0 w_1 w_2 ... w_n]$$

The output $y_j$ is equal to the inner product of $X_j$ and $W$

$$y_j = \left( X_j^T W \right)$$

The error $e_j$ is defined as the difference between the desired response $d_j$ and the actual response $y_j$

$$e_j = d_j - X_j^T W$$

In adaptive filtering applications the desired response is usually composed of some underlying signal to be estimated plus additive noise uncorrelated with both the signal and the filter input. Assume that the sequence of pairs $\left\{ \left\{ d_j, X_j^T \right\} \right\}_{j=1}^{\infty}$ is a stochastic process which need not be stationary. The expectations are taken over the ensemble described by this stochastic process. The correlation matrix at time $j$ as defined by

$$R_j = E \left[ X_j X_j^T \right]$$

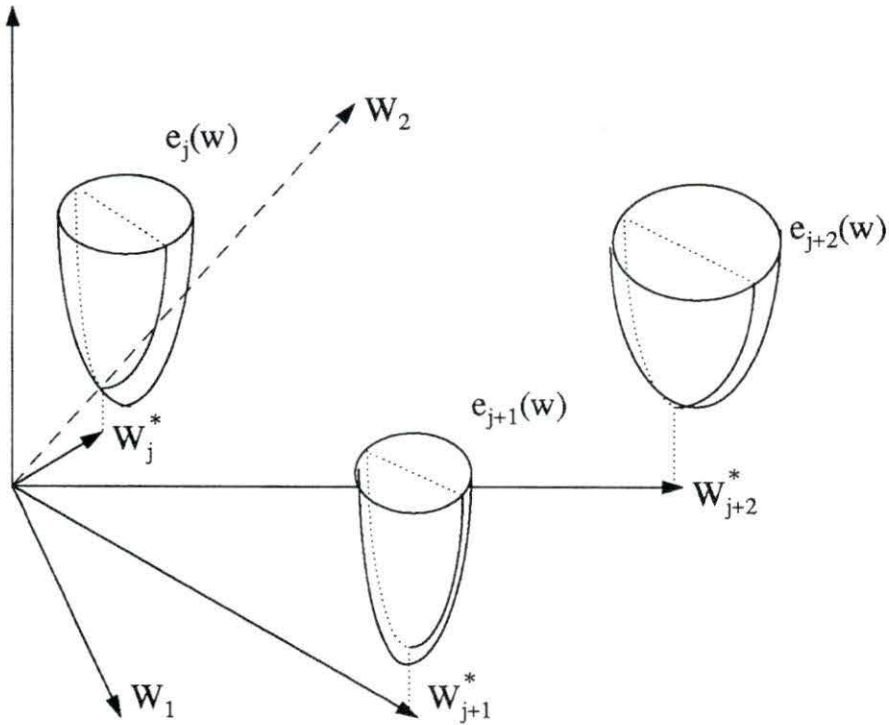is assumed to be positive definite. The cross-correlation vector is defined by

Figure 5.2:   Time Varying Error Surface

$$P_j = E\left[d_j X_j\right]$$

The mean square error at time $j$ is given by

$$e_j = E\left[d_j^2\right] - 2W_j^T P_j + W_j^T R_j W_j$$

The error surface is a quadratic function of the weight vector at any particular time and can be viewed as a concave hyperparaboloidal surface. With non-stationary inputs , the minimum point, orientation , and curvature of the error surface could be

changing over time as shown in Figure 5.2. If, however the desired signal and input signal vectors are jointly stationary then the statistics $R_j$ and $P_j$ are constant, and only a single error surface needs to be considered. In this case the gradient search method can be used to find the minimum. The Leaky LMS algorithm was adopted. $W_j$ can be found by the following recursive equation:

$$W_{j+1} = \beta W_j + 2\mu e_j X_j$$

Signals composed of recurring pulses in noise are highly non-stationary due to their time-varying statistical character. The LMS adaptive filter, which is able to track such rapidly varying non-stationarities, essentially converges to the best time-invariant filter.

### 5.2.1 Filter Description

The signals to be considered are those whose statistical properties recur at various points in time called regeneration times. It is required that the autocorrelation matrix $R_j$ and the cross-correlation vector $P_j$ at any particular time are elements of some finite set and they occur in identical sequence after each regeneration time. The times between regenerations are allowed to be variable. Thus the entire sequence of $R$ matrices and vectors will not in general be used each cycle, because the occurrence of regeneration starts the sequence over. There exists a sequence of error surfaces as show in Figure 5.2. The TSAF proposed uses a multiplicity of weight vectors usually one corresponding to each error surface. Since the number of different error surfaces for a statistically recurring processes is finite, the number of weight vectors is also finite. The weight vectors are denoted by $W_0, W_1, W_2...W_n$. At a time, only one weight

is selected, based on the error surface present at that instant and is adapted towards the minimum error surface. When the minimum surface is reached the weight vector is the Wiener weight vector (optimum weights obtained by the Wiener solution) for that error surface, yielding a minimum mean squared error filter at that 'station' at that time. Thus each weight vector becomes an expert in filtering a particular portion of the interval between regenerations. For this procedure an external input to the filter, called the sequence number $s_j$ is used to determine the appropriate weight which is used at time $j$. Thus when $s_j = i$ the $ith$ error surface is assumed to be present, so that the $ith$ weight vector is used to form the filter output and then adapted towards the bottom of the error surface. In order to set the sequence number some a priori knowledge of the filter input is required. For pulse type signals, apriori knowledge could be the location of the pulse in time. For signals with periodic statistics (sometimes referred to as cyclostationary) the knowledge of the period is sufficient. Mathematically the TSAF algorithm is

$$Y_j = X_j^T W_{sj}(j)$$

$$W_j(j+1) = W_j(j), i \neq s_j$$

$$W_j(j+1) = \beta W_j(j) + 2\mu e_j X_j, i = s_j$$

where $W_i(j)$ is the value of the $ith$ weight vector at time $j$. A different $\mu$ is used for each weight vector. This is done in order to keep the percent loss in the steady-state performance (due to the adaptive process referred to as misadjustment) the same for each weight vector. A conceptual block diagram of the TSAF is shown in Figure 5.1.

## 5.2.2 Disadvantages of the TSAF

In some applications, due to uncertainty in $s_j$ at any particular time, error is introduced at the output. The performance in the face of uncertainty in $s_j$ was analyzed by Ferrara [29]. If the sequence number can be chosen perfectly, then it can be shown that the TSAF converges to the optimal (minimum point of each error surface is reached) time-varying filter when the adaptation is performed slowly enough. Although in comparison with the LMS, the computational complexity is the same, the TSAF is an expensive approach to signal processing.

The number of data points required for the TSAF filter to converge to its time-varying solution is greater than that required for a conventional LMS based system. The memory requirement to implement this filter is large due to the multi-weight vectors (memory must be allocated to store the filter weights).

## 5.2.3 Typical Applications

The increased performance resulting in the time-varying solutions compensates for the disadvantages in the TSAF. One application of the time-sequenced filter was to fetal electrocardiography. The location of the fetal pulses in time must be estimated in order to synchronize the filter time-varying impulse response to the fetal cardiac cycle. The TSAF can also be used to predict future samples of a stochastic process which has a periodic nature. The load prediction problem was studied in [30] by Ferrara. Power consumption exhibits a clear daily cycle. The actual demand during a particular hour varies from day to day. The TSAF can be used as a predictor to predict power consumption one-half hour to one week in the future based on past values.

## 5.3   Proposed Scheme to Detect Late Potentials

The late potentials are modeled as described in Chapter 6. The late potentials are then added to the $R$ wave of the QRS and allowed to decay into the ST segment. Two separate channels are required. The channels have correlated signal components but uncorrelated noise components. A leaky LMS algorithm which was found to yield a high SNR in comparison with the conventional LMS (other adavantages of the leaky LMS are discussed in [27]), was used to find the weights.

Figure 5.3 describes the proposed scheme. In both channels, the $X$ lead data was used. White noise from two different sources was added to both the channels. Synthesized late potentials were added to both the channels. It is assumed that the electrodes are placed close together, but far apart so that the muscle noise in both the channels is uncorrelated. The sequence number used is the $R$ wave. The TSAF requires knowledge and location of the Late potentials. This information is available from a $R$ wave detector that was designed. The error in the $R$ wave detector was approximately $3msec$. The data was sampled at 1000 Hz and the regeneration times were from around $500msec$ to $650msec$ in the QRS waveform. Simulations were performed for different tap sizes and different $\mu$ for the Leaky LMS algorithm. The results are discussed in Chapter 6.
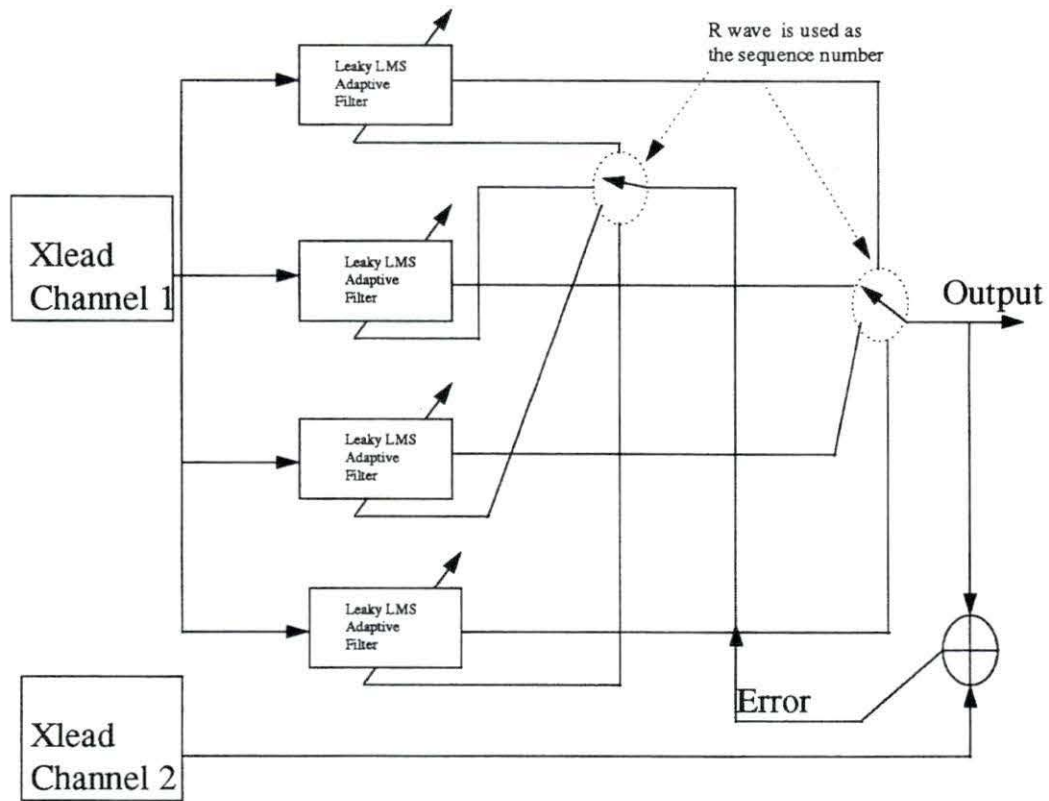
Figure 5.3:   Proposed TSAF to Detect Late Potentials

# CHAPTER 6.   SIMULATION RESULTS

## 6.1   Data Acquisition

The data were acquired through a commercial signal averaged ECG device. The data was sampled at 1000Hz and had a resolution of $1.25\mu v/bit$. The data contained about 15 minutes worth of raw ECG from the three orthogonal leads. Data are made available from two patients. The first set of data was used as control and the other as the VT inducible case. Signal averaged data was also acquired from a database. This database consisted of 18 patients. The data contained only signal averaged ECG's, i.e., one QRS beat for each of the $XYZ$ lead and about 600 samples long and the data was sampled at 1000Hz. The data are only used to create and test the signal averaged ECG i.e. calculation of QRS endpoint and actual detection of late potentials. The four pole Butterworth filter was applied to this data and the RMS value was calculated and compared with results available in the database. Typical $XYZ$ lead data are shown in Figure 6.1.
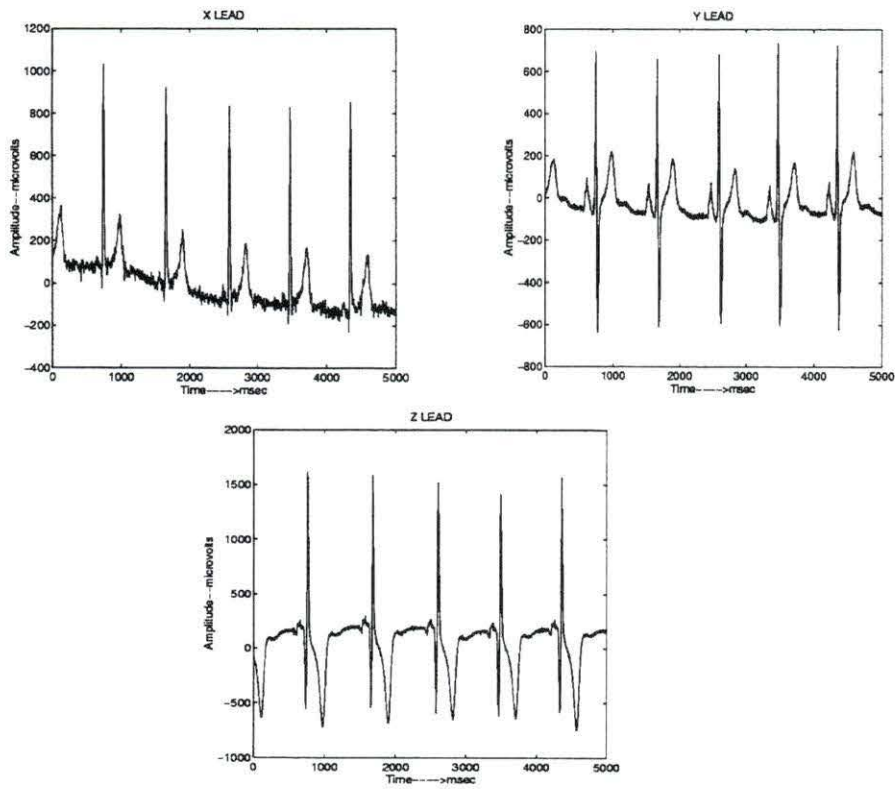
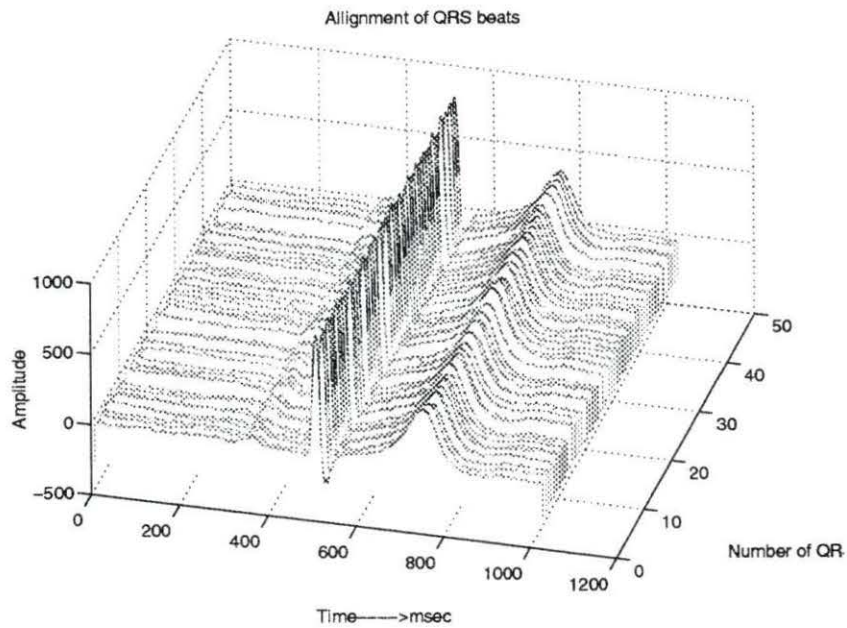Figure 6.1: The Three Orthogonal Leads X Y and Z

Figure 6.2:   Time Averaging

## 6.2   Simulation methods

### 6.2.1   Signal Averaging

The data were aligned using a QRS detection algorithm [26]. The $R$ wave was used to align the beats. Ectopic (noisy) beats were rejected. A typical time average after the $R$ wave detection is shown for the $X$ lead in Figure 6.2.

After the time averaging is done, the data is passed through a 4 pole Butterworth filter. The data is filtered to the QRS midpoint and then filtered in the other direction as described in Chapter 2. The filter bandwidth was set to 40-250Hz. The results

are shown in Figure 6.3.

### 6.2.2  LMS and Leaky LMS

The data for the three leads is passed through an adaptive line enhancer. The data was first scaled (by 1000) before it was passed through the filter. Both the LMS and the leaky LMS algorithm was run on the filter. Simulations were carried out for different filter tap sizes and different step sizes. The optimum filter length was found to be 64 taps and the value of $\mu$ and $\beta$ for the leaky LMS were approximately .099 and .06 respectively. These values were obtained by trial and error. Figure 6.4 compares the signal average, LMS and leaky LMS for the $X$ $Y$ and $Z$ lead. The leaky LMS algorithm was also run on the Motorola 56K. The data was scaled before it was input to the fixed point DSP. The scaling factor was 1000 so that the data fell in the range of $\pm 1$. The output of the LMS based adaptive filter clearly shows reduction of the beat-to-beat noise level. In Figure 6.4 (X lead data), the performance of the Leaky LMS algorithm yields lower noise levels on a beat-to-beat basis in comparison to the LMS. Similar results were observed for all the other orthogonal leads. The root mean square value was calculated and compared. The RMS values obtained by signal averaging before and after the LMS algorithms are shown in Figure 6.7. The RMS was evaluated on a beat-to-beat basis to show the feasibility of the algorithm. This is shown in Figure 6.8. The RMS value shows a clear reduction in the beat-to-beat noise level.

The noise figure qualifies the SNR. This noise figure is used to show that there was significant improvement in the SNR after adaptive filtering. Literature showed inconsistencies in defining a time segment to calculate the noise figure. A comparison
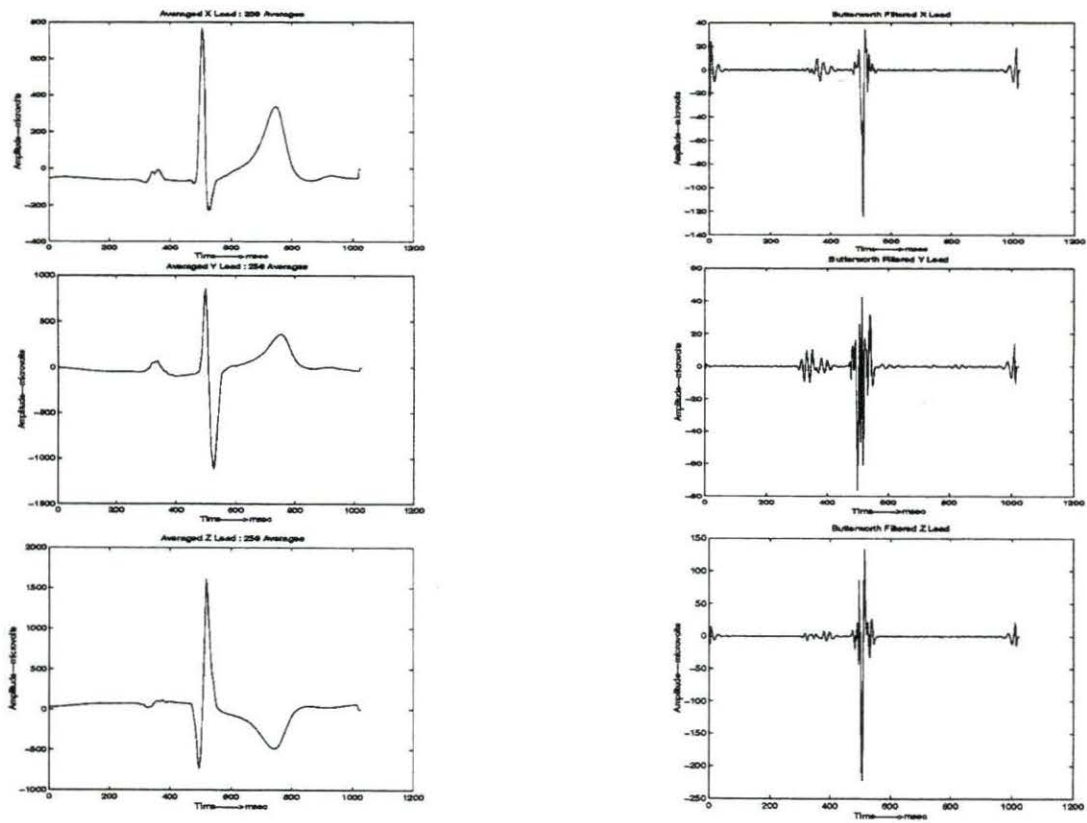
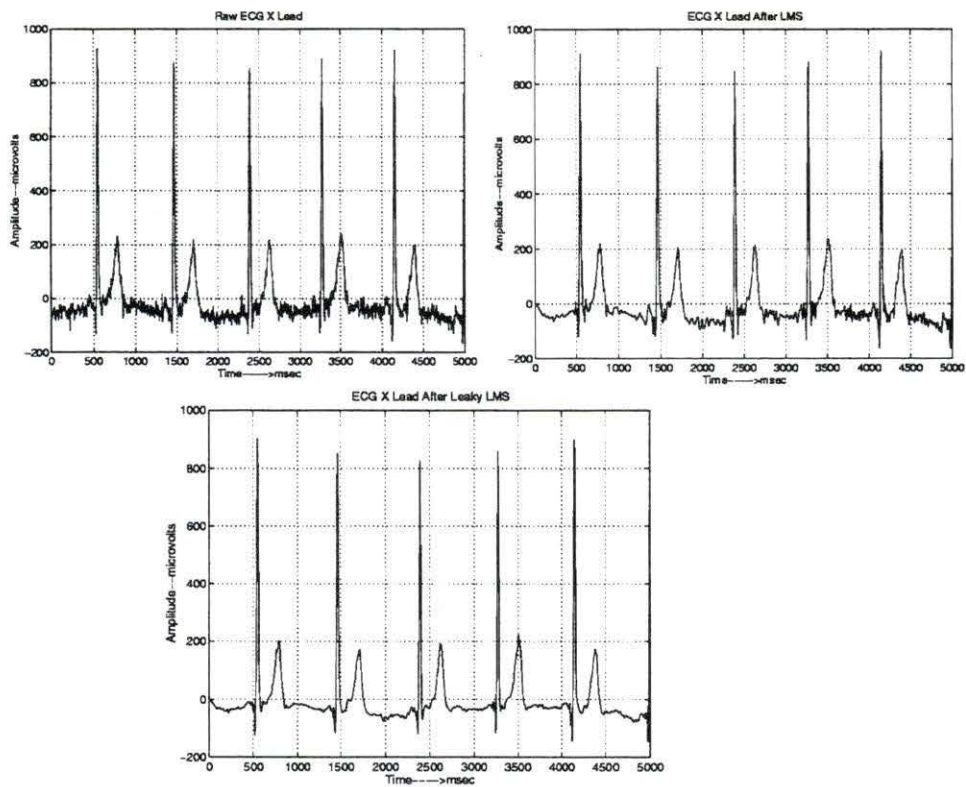Figure 6.3: The Orthogonal Leads and the Corresponding Butterworth Filtered Outputs

Figure 6.4: The X Lead: Raw X Lead, Output of LMS Based Adaptive filter and the Output of the Leaky LMS Based Adaptive filter
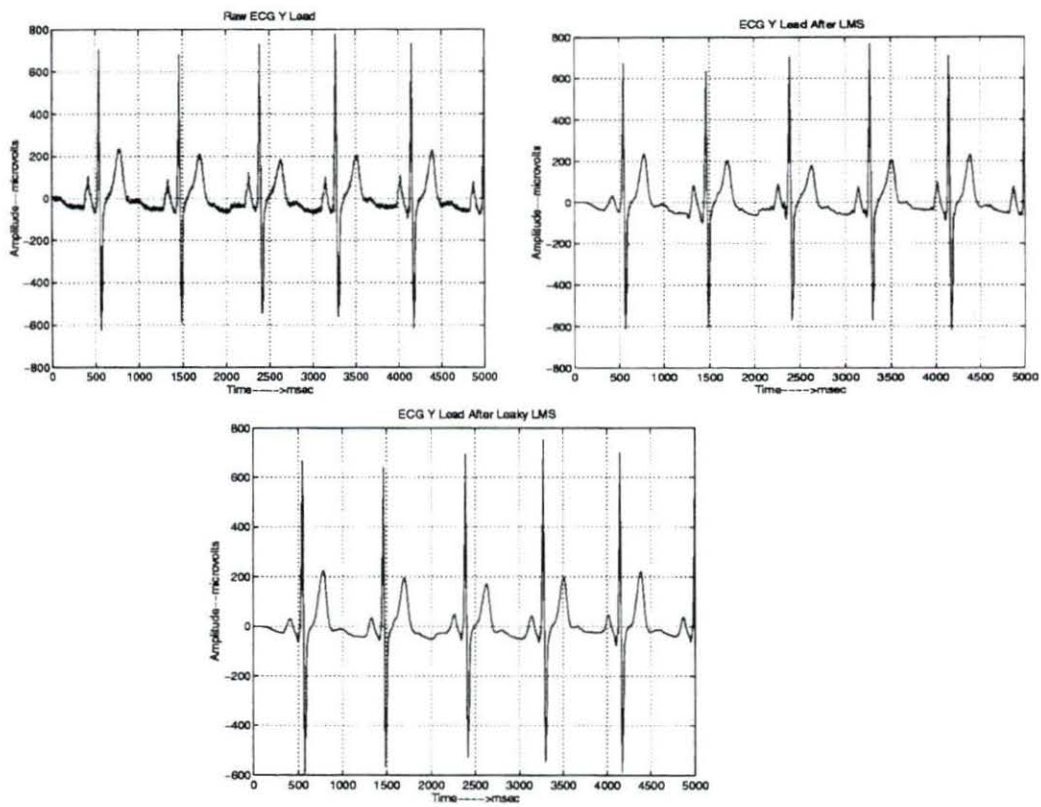
Figure 6.5: The Y lead: Raw Y Lead, Output of the LMS Based Adaptive Filter and the Output of the Leaky LMS Based Adaptive Filter
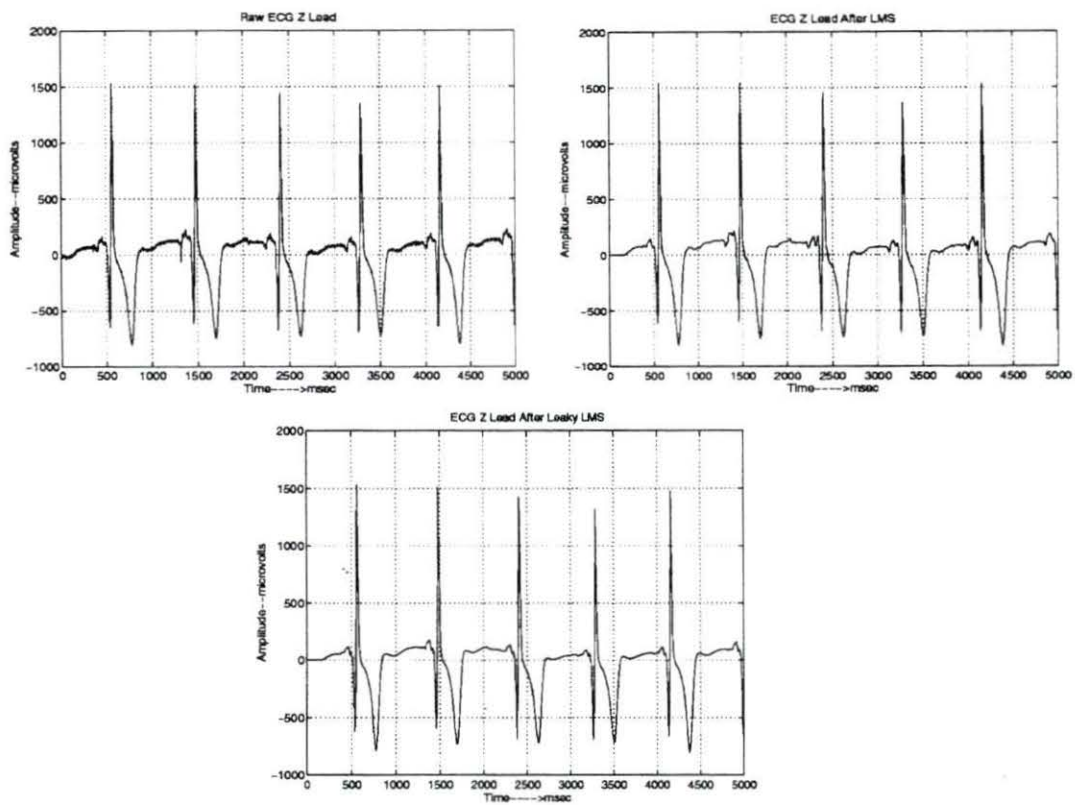
Figure 6.6: The Z lead: Raw Z Lead, Output of the LMS Based Adaptive Filter and the Output of the Leaky LMS Based Adaptive Filter
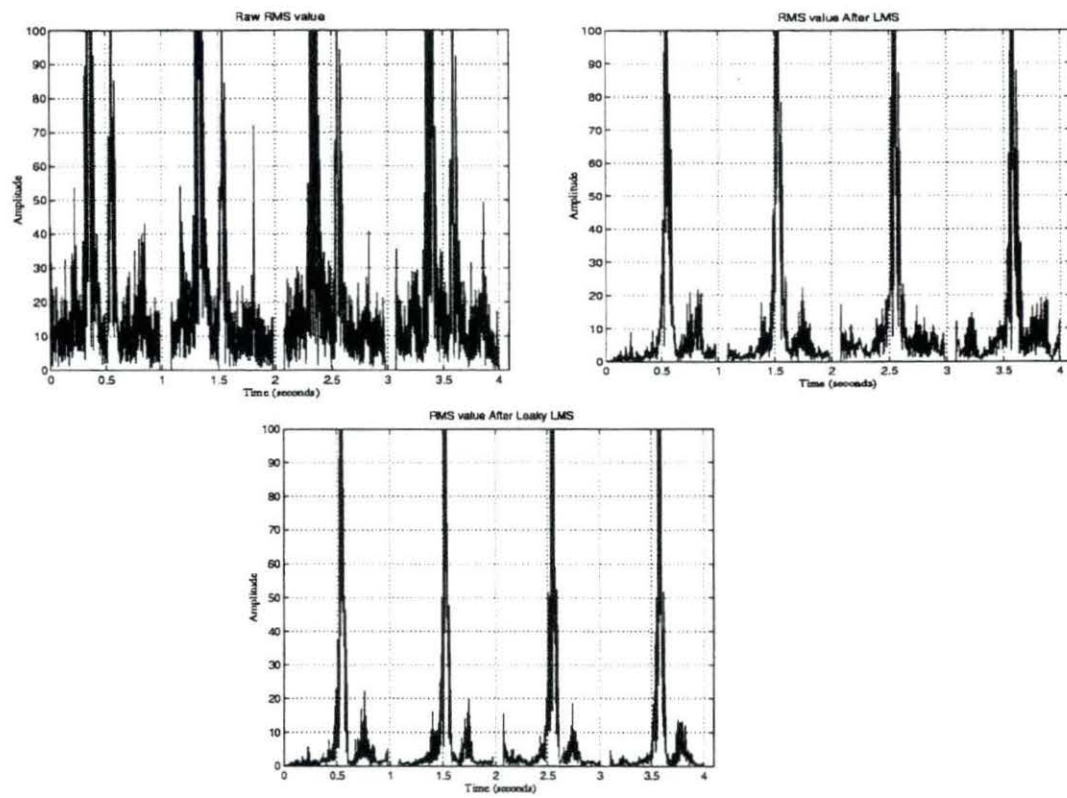
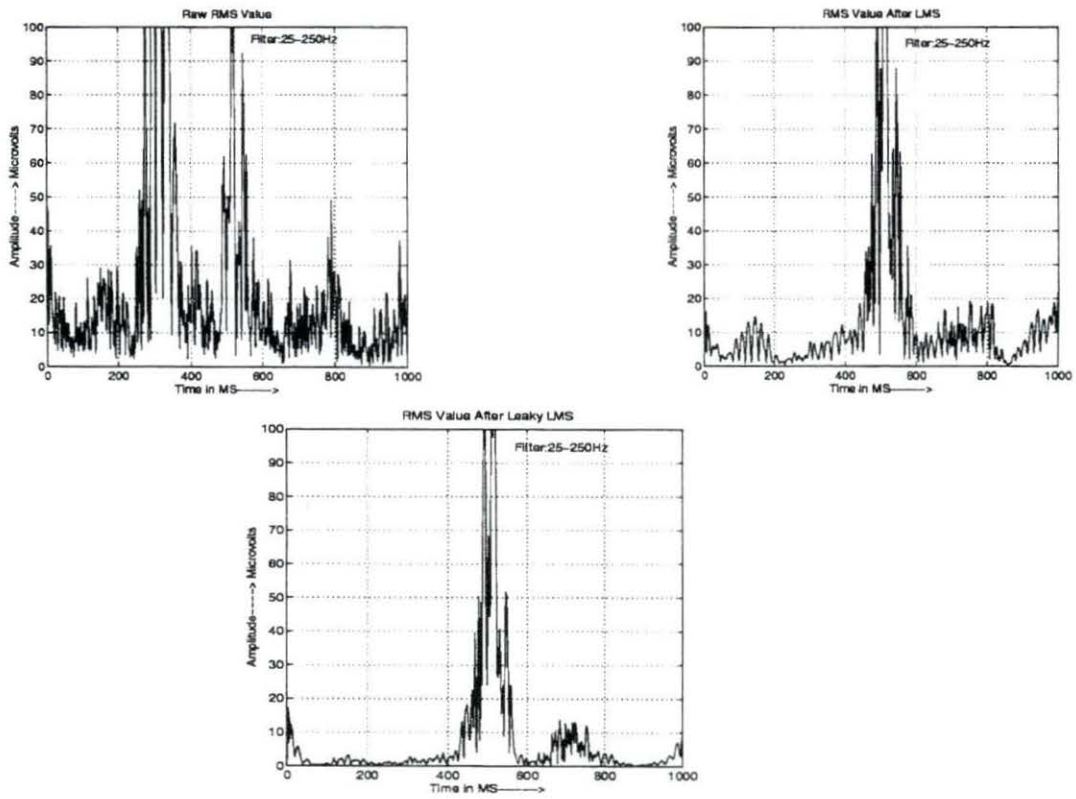Figure 6.7: RMS Value Comparison Before and After Adaptive Filtering

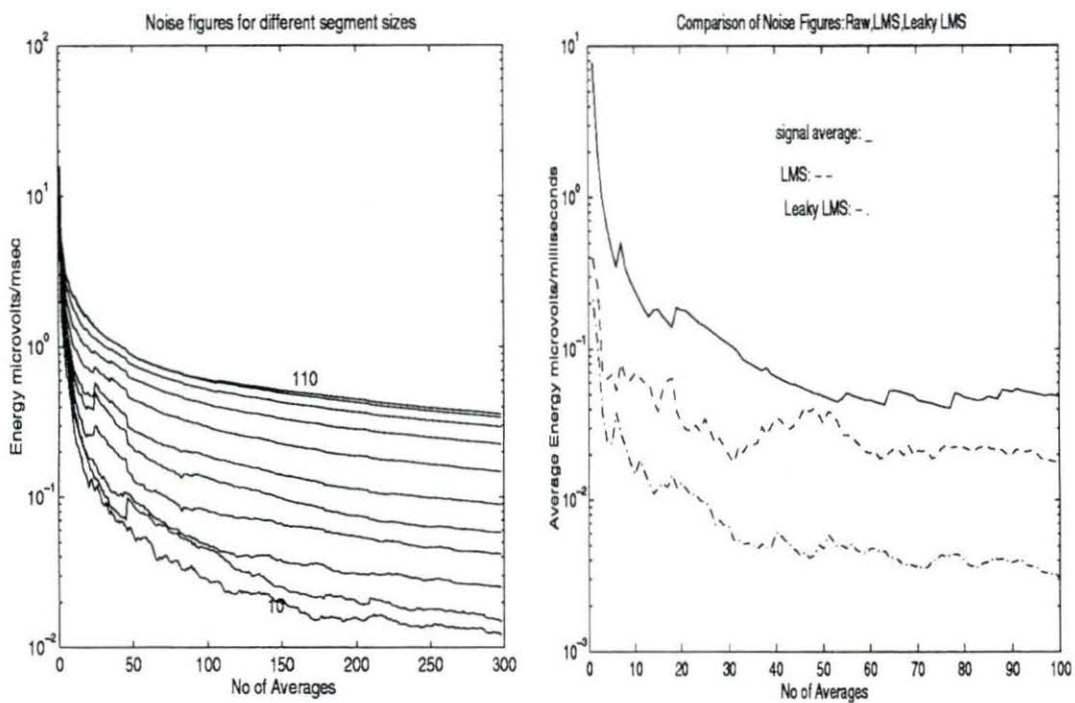Figure 6.8: The Beat-to-Beat Estimate of the RMS Value After Adaptive Filtering (LMS and Leaky LMS)

Figure 6.9: Comparison of Noise Figures for Different Time Lengths and Comparison in the performance of the Existing Technique to the Adaptive Filtering Technique

was made for different time segments as shown in Figure 6.9. The noise figures for the three methods were also compared. The noise figures after the leaky LMS was significantly low. This shows that the Leaky LMS algorithm can be used to detect beat-to-beat late potential detection technique. Figure 6.8 shows the vector magnitude when only one averaging was done. The noise seen after the ST time segment is very high (close to $20mVolts$ in the raw vector magnitude). After doing 256 averages the noise after the ST time segment is reduced to $0.5 - 2\mu Volts$. The recommended noise level is less than $0.3 \ \mu Volt$. The data from the orthogonal leads were then passed through the adaptive filter and the results showed an improvement in the SNR. Figure 6.8 shows the result of one averaging after the adaptive filter. The noise floor was already down to about $0.5\mu$Volts. After 2 averages, the noise floor was less than the recommended $0.3\mu Volts$ as seen in Figure 6.9 for the Leaky LMS algorithm based adaptive line enhancer. The results are significant since late potentials can be detected on a beat-to-beat basis (real time) because the noise floor is small. This would allow the detection of variability in late potentials. This result can be used to observe changes in the late potential activity when different drugs are administered to the patient. Researchers [24] are still in the process of formulating specific criteria to identify late potentials on a beat to beat basis.

## 6.3  Dynamic Time Warping

Dynamic time warping is recommended only when the QRS beats need to be averaged. Simulations were done with the asymmetric and symmetric algorithms proposed in [28]. The results are significantly different from results one would obtain from aligning speech samples. Simulations showed that it was best to use the

asymmetric form. There were two cases observed during averaging. The first case is when no QRS detection algorithm is used. This is demonstrated in Figure 6.10. The second case in Figure 6.11 shows that a QRS detector is used and then the peaks are aligned. However the beats are different due to the variability inherent in the QRS. The DTW technique works well when there are no prominent peaks observed in the signal. Warping becomes complex when distinguishing features (like the $R$ wave) are present in the ECG signal. Figure 6.12 illustrates the averaging procedure and shows that synthesized late potentials are not attenuated due to signal averaging. The results show that time axis fluctuations are removed and coherent averaging does not affect the amplitude of late potentials. Hence the warping technique is superior to the conventional averaging scheme which does not account for the variability of the late potentials. Simulation results show that warping works well in cases in which peaks are not aligned (Figure 6.10) and in cases in which (Figure 6.11) the peaks are aligned before warping. Thus the R-R interval detector can be avoided before time averaging. The warping has the disadvantage that a large memory space is required to store the reference samples and the path matrix. To simplify computation it was proposed that the beats be warped only in the $150msec$ before the ST segment. This is the region where late potentials are observed. However this technique would require different identification criteria as Simson's method cannot be used to detect late potentials. To illustrate this effect of warping on $150msec$ segments, simulations were carried out after averaging the beats. A typical [8] $sin(x)/x$ model was used to illustrate this effect. The results are shown in Figure 6.12 for 10 averages.
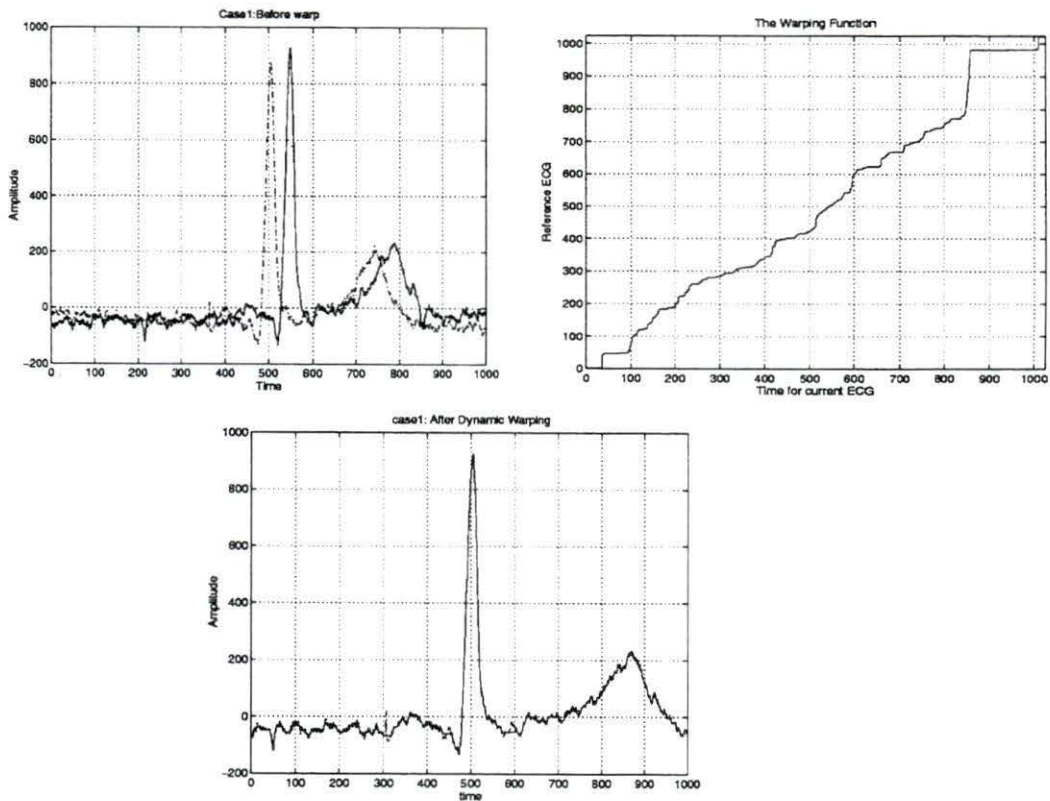
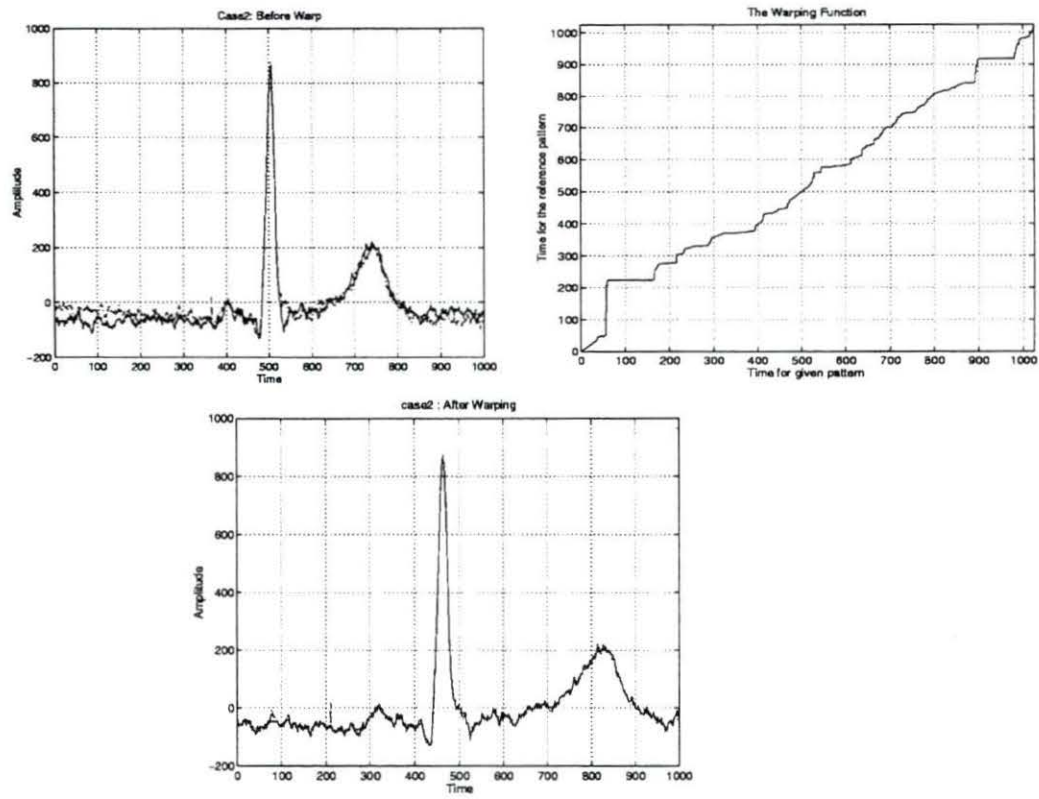Figure 6.10:   Case1: The Peaks are not Aligned

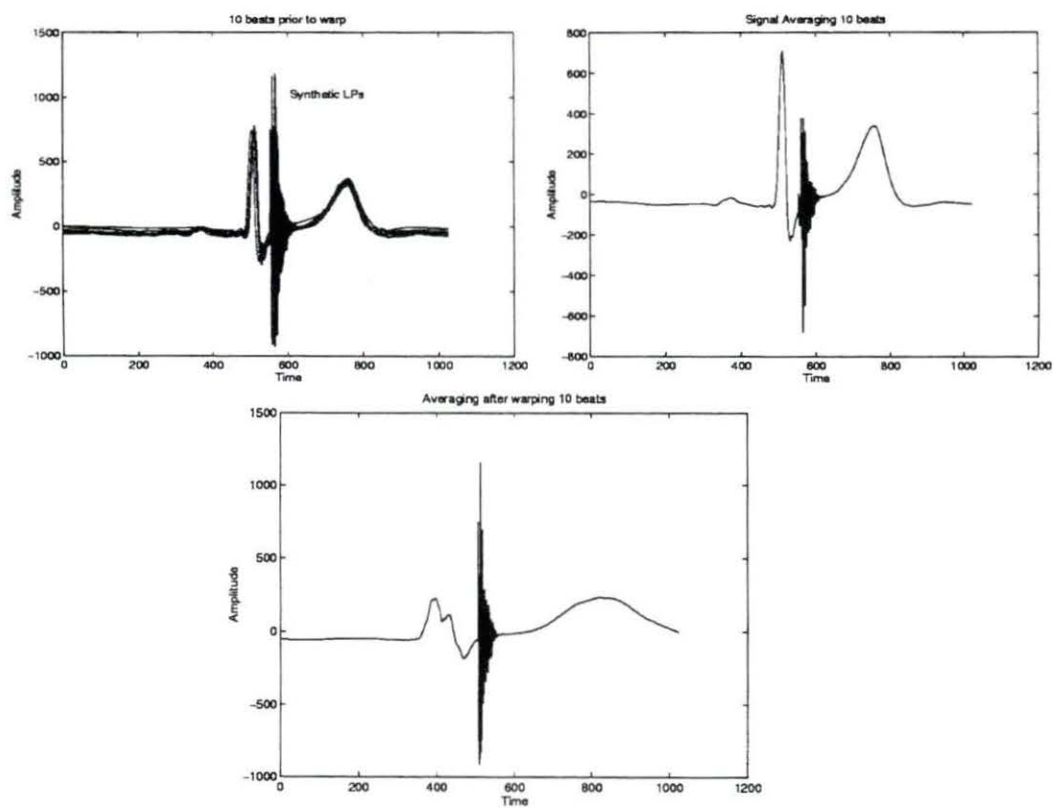Figure 6.11:  Case2: The Peaks are Aligned and then Warped

Figure 6.12: The Effects of Warping

## 6.4 Modeling Late Potentials

The late potentials are modelled as a 25 Hz sine wave in [14]. In [8] the late potentials are modelled as a decaying $sin(x)/x$ function having an amplitude of $20\mu V$ and frequency of 40-200 Hz. Models that represent the actual statistics of the signal have not been described in literature. The following model is proposed for the late potential as a realization of the random process. The Figure 6.13 shows that white noise of unity variance is fed into the system modelled by two AR coefficients and modulated by a decaying exponential (typically $e^{-\frac{1}{10}t}$ ). The model is valid as it displays characteristics shown by late potentials. The time varying nature was incorporated by adding late potentials at different times after the QRS for different beats.

## 6.5 Time Sequenced Adaptive filtering

Simulations were carried out for TSAF by using the $X$ lead data. The late potentials generated from the above models were added to the ECG $40msec$ after the presence of the $R$ wave. The late potentials were generated at random times and they decayed into the ST segment. The idea is to use two $X$ lead channel ECG signals. The electrodes must be kept as far apart as possible so that the noise in both the leads is uncorrelated. This was achieved by taking the $X$ lead and branching them off as two channels by adding white noise from two different sources. The data was then passed through a TSAF. The TSAF consisted of a bank of 4 adaptive filters. The $R$ wave was used as the sequence number. The first filter filtered the data until the end of the $R$ wave. The second and third bank of filters filtered the data
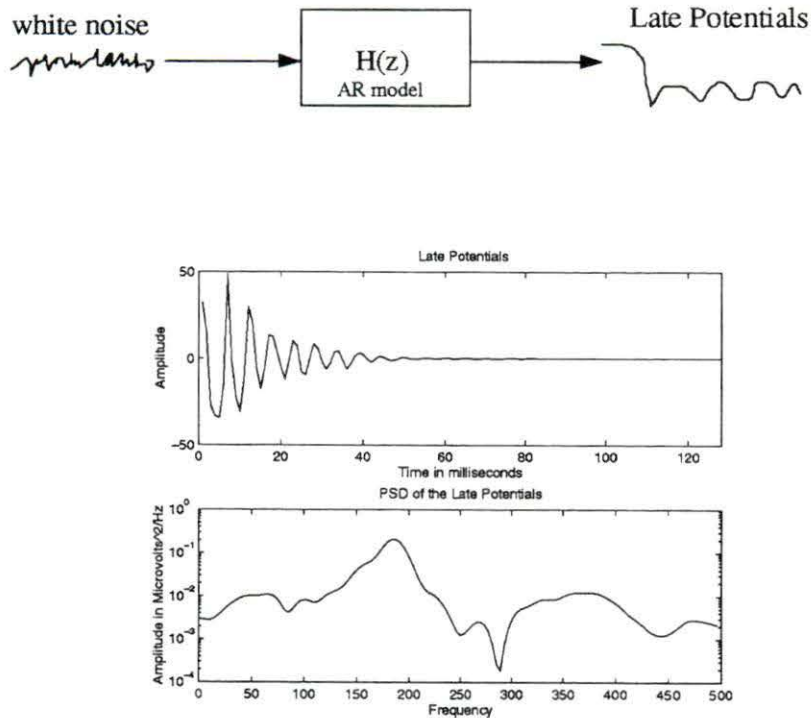
Figure 6.13:   Model of Late Potentials

until the beginning of the ST segment and the last filter filtered the ST segments. Different tap sizes and different $\mu's$ were used for the filter. Figure 6.14 illustrates the output of the filter after 100 beats. The problem with this filter is that a large data segment needs to be passed through the filter before it can act as a time varying filter. This concept was indicated by Ferrara [30]. The filter works better than the regular adaptive line enhancer which will not detect time varying signals. This technique of using the TSAF to detect late potentials facilitates the detection of late potentials on a beat-to-beat basis without needing to calculate the RMS value. This filter can be used to track the variability of the late potentials over a 24 Hr period and the results
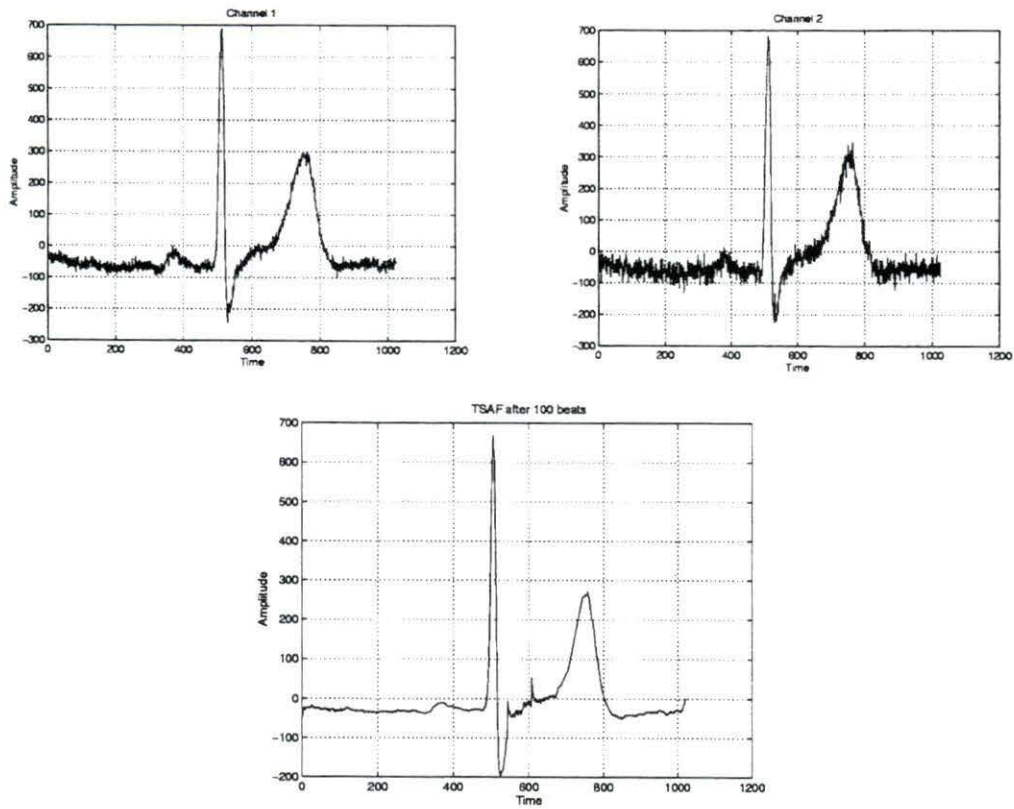
Figure 6.14:   The Two Input Channels and the Output of the TSAF

will be clinically significant. The study is based on preliminary research results and real patient data are needed to achieve statistical significance.

## CHAPTER 7.    CONCLUSIONS

Simulations show that there is a good agreement with clinical observation of late potentials and the results demonstrate significant improvement in the SNR after adaptive filtering. This improvement in SNR shows that adaptive filtering can be used to detect the late potentials on a beat-to-beat basis. The time required to compute the RMS value is approximately 2-10 seconds as compared to the existing SAECG techniques that take about 5 minutes. This technique is easily realized in real time and this was demonstrated by running the program on a 56K simulator. Late potential variability can be tracked and it may be used to improve classification of SAECG. Even though the preliminary study here suggests good results, it is acknowledged that more data will be needed from patients with different symptoms (left bundle branch block (LBBB), RBBB etc.) to test the performance of the real time system. Preliminary research results show that the time sequenced adaptive filter can be used to track the late potential variability on a beat-to-beat basis. To achieve any statistical significance, real data from patients suffering form different abnormalities are needed. There is a need for a process for formalizing specific criteria for identification of late potentials on a beat-to-beat basis.

# BIBLIOGRAPHY

[1] E. Berbari and P. Samet, "Non invasive technique for detection of electrical activity during the PR segment," *Circulation*, pp. 1005–1043, 1973.

[2] N. El-Sherif, ed., *High Resolution Electrocardiograph*. Futura Publishing Company, Inc., New York, 1992.

[3] R. H. E.Berbari, B. Scherlag and R. Lazzara, "Recording from the body surface of arrhythmogenic ventricular activity during the ST segment," *Am.J.Cardiol.*, pp. 697–702, 1978.

[4] M. Simson, "Use of signals in the terminal QRS complex to identify patients with ventricular tachycardia after myocardial infarction," *Circulation*, pp. 235–242, 1981.

[5] D. Coast, "Analysis of beat-to-beat late potential variability and the effect of atrial pacing," *Computers in Cardiology*, 1994, (in press).

[6] N. Flowers, "The anatomic basis for high frequency components in the electrocardiogram," *Circulation*, pp. 531–539, 1969.

[7] A. M.Katz, *Physiology of the Heart*. Raven Press Books, Ltd., New York, 1977.

[8] C. Spiers, "Bispectral analysis for the detection of ventricular late potentials," *Computers in Cardiology*, pp. 427–430, 1993.

[9] P. Gardner and P. Ursell, "Electrophysiologic and anatomic basis for fractionated electrograms recorded from healed myocardial infarcts," *Circulation*, pp. 596–611, 1985.

[10] M. Simson, "Clinical applications of signal averaging," *Cardiol.Clinics*, pp. 109–119, 1983.

[11] N. Sherif and R. Mehra, "Appraisal of a low noise electrocardiogram," *J.Am.Coll.Cardiol.*, pp. 456–467, 1983.

[12] S. Jesus and H. Rix, "High resolution ECG analysis by an approved signal averaging method and comparison with a beat-to-beat approach," *Journal of Biomedical Engineering*, pp. 25–32, 1988.

[13] M. B.Shelton, "A system for high resolution electrocardiography," *University of Minnesota*, pp. 1–16, 1987.

[14] F. Tuter, *Wavelets:Time-Frequency and Phase Space*. Springer-Verlag, Ltd.,New York, 1989.

[15] P. Lander and P. Gomis, "Modeling abnormal signals within the QRS complex of the high resolution ECG," *Computers in Cardiology*, pp. 435–437, 1992.

[16] E. Chan, "Autoregressive estimation of closely-spaced spectra in the late potential region of the signal averaged electrocardiogram as a function of segment width and ST slope," *Computers in Cardiology*, pp. 71–74, 1992.

[17] R. Attarinejad and L. Sornmo, "Maximum liklehood analysis of late potentials," *Computers in Cardiology*, pp. 67–70, 1992.

[18] H. AL-Nashash and S. Kelly, "Non invasive beat-to-beat detection of ventricular late potentials," *Medical and Biological Engineering and Computing*, pp. 64–68, 1989.

[19] W. Wang and M. English, "Technique for real-time beat-to-beat recovery of microvolt cardiac signals," *Computers in Cardiology*, pp. 413–416, 1992.

[20] L. Shelton, "Detection of late potentials by adaptive filtering," *Journal of Electrocardiology*, pp. 138–143, 1985.

[21] C. Spiers, "Least squares time sequenced adaptive filtering for the detection of fragmented micropotentials," *Computers in Cardiology*, 1994 (in press).

[22] S. Chen, "Prony residual anaysis for the identification of cardiac arrythmias," *ICASSP 95*, 1995 (in press).

[23] A. Gomes, ed., *Signal Averaged Electrocardiography.* Kluwer Academic Publishers, New York, 1993.

[24] "Standards for analysis of ventricular late potentials using high-resolution or signal averaged electrocardiography," tech. rep., American College of Cardiology, 1991.

[25] G. Friesen, "A comparison of the noise sensitivity of nine QRS detection algorithms," *IEEE Transactions of Biomedical Engineering*, pp. 85–97, 1990.

[26] P. Tompkins, "A real time QRS detection algorithm," *IEEE Transactions in Biomedical Engineering*, pp. 66–72, 1970.

[27] B. Widrow and S. Stearns, *Adaptive Signal Processing*. Prentice-Hall, Inc., New York, 1985.

[28] H. Sakoe and S. Chiba, "Dynamic programming algorithm optimization for spoken word recognition," *IEEE Transactions on ASSP*, pp. 43–47, 1978.

[29] E. Ferrara and B. Widrow, "The time sequenced adaptive filter," *IEEE Transactions in ASSP*, pp. 679–683, 1981.

[30] E. Ferrara and B. Widrow, "Fetal electrocardiogram enhancement by time sequenced adaptive filtering," *IEEE Transactions on Biomedical Engineering*, pp. 458–460, 1982.